Utrecht University

Institute for Theoretical Physics

Masters Thesis

Anomalous Transport from Dynamical Gauge Fields and Holography

Author
Eamonn Weitz

Supervisors
Dr. Umut Gürsoy
Dr. Matti Järvinen

January 15, 2020

Abstract

Since the inception of quantum anomalies in the 1960's, the topic has come to be generally quite well-understood. Nonetheless, it is still not clear how exactly anomalous effects can be observed on a macroscopic scale within the context of particle physics. Through hydrodynamic considerations, one finds that certain anomalies could macroscopically produce what is known as anomalous response, a process giving rise to $\mathcal{P}$-odd, $\mathcal{T}$-even transport phenomena. The associated anomalous conductivities have been computed in the absence of dynamical gluons using a variety of approaches, which have lead to the belief that the conductivities obey a universality restriction. We attempt to compute radiative corrections to such universal values by including dynamical gluons within the setting of the quark gluon plasma. Due to the difficulty of studying quantum chromodynamics using perturbation theory, we compute the conductivities using a holographic model, namely V-QCD. Our model recovers the universal values of the conductivities in the absence of dynamical gluons. After including such dynamical effects, we observe no radiative corrections to the Chiral Magnetic Effect or Chiral Vortical Effect. However, we find that the Chiral Separation Effect does recieve radiative corrections.

Contents

Chapter 1

Introduction

Noether's theorem says something very deep, yet simple about symmetry. While the connection it provides between the symmetries of a physical system and conserved quantites can be understood by a high school student, its consequences for quantum systems are much more subtle. It turns out that symmetries that are respected classically are not always so lucky upon quantization. We will now specify as to what exactly is meant by this.

In even spacetime dimensions the Lorentz group has two unitarily inequivalent spinor representations, giving rise to the notion of chirality. On a classical level Noether's theorem implies that for a chirally symmetric theory, i.e a theory with massless fermions, there exists an associated conserved axial current. However, one has to be mindful when considering chiral transformations in the quantized theory. In particular, one finds that the path integral picks up a non trivial Jacobian under chiral transformations, which implies the presence of a chiral anomaly.

As long as we are speaking of a global symmetry there is no issue and the anomaly is nothing more than a feature of the quantum theory. Indeed, the existence of chiral anomalies in particle physics is experimentally validated by the observation of a neutral pion decaying into two photons [1], a process, which is prohibited by the classical theory. Be that as it may, the gauging of an anomalous symmetry leads to a violation of unitarity. Consequently, anomaly cancellation is imposed on gauge theories, which in the case of the standard model greatly contrains its fermion content.

The goal of this thesis is to study possible macroscopic manifestations of quantum anomalies, specifically in systems possessing chiral fermions. Through the study of parity-odd ($\mathcal{P}$-odd), time reversal-even($\mathcal{T}$-even) transport in the context of hydrodynamics, one identifies a plethora of so-called anomalous conductivites giving rise to what is known as anomalous transport. Anomalous transport phenomena are thought to play role in many different fields of physics. In condensed matter, they are relevant in the study of Dirac and Weyl semimet-

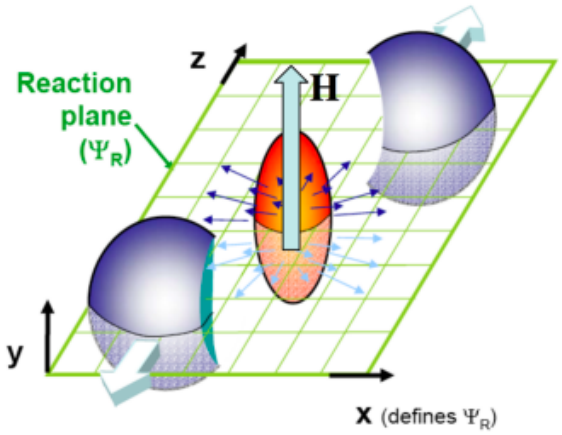

Figure 1.1: Illustration of the creation of the QGP taken from [2]. Relativistic heavy ions are collided producing hot QCD matter, which is penetrated by a strong magnetic field, $\boldsymbol{H}$.

als [3]. It has been suggested in astrophysics that anomalous transport is responsible for the sudden acceleration of neutron starts at birth [4], known as neutron star kicks. Furthermore, such phenomena have been invoked [5] in an attempt to explain charge asymmetries in the final state of heavy ion collisions [6]. It is the latter example, which we will focus on in this thesis.

The sole existence of a quantum anomaly is not enough to produce anomalous transport; it is necessary that we consider our theory of interest on a chiral medium. This provides a hint as to why we might observe anomalous transport in the quark gluon plasma (QGP), the phase of quantum chromodynamics (QCD) where deconfined quarks can be modelled as a chiral fluid. As shown in Fig 1.1, experimental access to the QGP is provided by the collisions of relativistic heavy ions. If the impact parameter in non-zero, an intense magnetic field will be created that is aligned, on average orthogonal to the reaction plane.

Strongly coupled gauge theories such as QCD are notoriously difficult to work with using perturbative methods. Therefore, it is necessary to make use of nonperturbative techniques. A prime example of the latter is holography, which has been identified as an important tool in studying anomalous transport phenomena [7], [8]. In this thesis, we will make use of holography to compute anomalous conductivities in the presence of dynamical gluons. The thesis is outlined as follows.

In Chapter 2, we will discuss how anomalous transport arises in the context

hydrodynamics. We will also define the individual chiral conductivities and list their universal values. Chapter 3 will firstly review anomalies from a microscopic perspective before qualatively explaining the macroscopic anomalous effects in a QGP background. We will use 4 to introduce holography and specifically, the AdS/CFT correspondence. Moreover, we will define a holographic model, which we use to study the QGP, namely V-QCD.

The final two chapters will consist of the results. In particular, Chapter 5 will contain details of the holographic background to be considered. In addition, we will note the consequences of the inclusion of a massive vector field in the bulk theory. Linear response will then be performed on this background in Chapter 6 and the relevant anomalous conductivities will be computed. Lastly, a conclusion and outlook section 7 are included summarizing the work of the thesis and suggesting future research directions.

Chapter 2

Hydrodynamics

Laboratory experiments are often performed by perturbing some equilibrated system with an external source, Φ_0^A coupled to an operator $\mathcal{O}^B$, before observing said response $\delta\langle O^B\rangle$ to such a perturbation. Through linear response theory, we study such a response at linear order in the external source [9]. In Fourier space, this is expressed as

$$\delta\langle O^B\rangle = G_R^{BA}\Phi_0^A, \tag{2.1}$$

where G_R^{BA} is the retarded Green's function

$$G_R^{BA}(k) = -i\int d^4x e^{-ikx}\Theta(t)\langle[\mathcal{O}^A(t,x),\mathcal{O}^B(0,0)]\rangle, \tag{2.2}$$

with $\theta(t)$ a step function. As we will see below, such a response is characterized by transport coefficients. Transport coefficients are then determined by Kubo formulae, which are stated in terms of the Green's functions. The main goal of this thesis will be to calculate such transport coefficients.

These aforementioned Green's functions should be determined from the microscopic theory, which in our case is QCD. However, the QGP phase of QCD is a strongly coupled fluid and thus cannot be studied using conventional perturbative techniques. Nonetheless, these Green's functions can in some cases be computed using the AdS/CFT correspondence, as we will see in Chapter 4. On the other hand, one can narrow down the necessary information concerning the Green's function using macroscopic considerations such as conservation laws and low-energy effective theory. The latter formalism is known as hydrodynamics.

2.1 Constitutive Relations

Hydrodynamics is an effective field theory describing the time evolution of systems near equilibrium [10]. Such a description directly concerns currents asso-

ciated with the microscopic theory, whose equations of motion are identified as the Ward identities evaluated from the quantum theory. Next, one writes down the so-called consitutive relations, which are intended to capture phenomenologically the macroscopic properties of the system of interest. These are given in terms of locally defined thermodynamic quantities such as temperature, T and chemical potential, μ. For the $U(1)$ vector current, axial current and the energy-momentum tensor these are

$$\langle J_a^\mu \rangle = \mathcal{N}_a u^\mu + j_a^\mu \quad , \quad a = (V, A), \tag{2.3}$$

$$\langle T^{\mu\nu} \rangle = \mathcal{E} u^\mu u^\nu + P\Delta^{\mu\nu} + (q^\mu u^\nu + q^\mu u^\nu) + t^{\mu\nu} \tag{2.4}$$

respectively, where u^μ is the fluid velocity, $\Delta^{\mu\nu} = \eta^{\mu\nu} + u^\mu u^\nu$ and j_a^μ, q^μ are transverse to the fluid velocity [11]. The coefficients $\mathcal{E}$, P, $\mathcal{N}_a$, q^μ, j_a^μ and $t^{\mu\nu}$ will be given in terms of T, μ_V and u^μ. Note that for the moment, the above two equations are just the general decompositions of a symmetric 2-tensor and a vector in flat spacetime. However as hydrodynamics is concerned with states deviating slightly from thermal equilibrium, it assumes a priori that the local thermodynamic quantities $T(x)$, $\mu_V(x)$ as well as $u^\mu(x)$ are slowly varying functions. With this assumption in mind, we can organize the constitutive relations in a derivative expansion of x,

$$\langle J_a^\mu \rangle = \langle J_a^\mu \rangle_{(0)} + \langle J_a^\mu \rangle_{(1)} + ..., \tag{2.5}$$

$$\langle T^{\mu\nu} \rangle = \langle T^{\mu\nu} \rangle_{(0)} + \langle T^{\mu\nu} \rangle_{(1)} + ... \tag{2.6}$$

In this thesis we will only be concerned with the first two terms in the derivative expansion [1].

At zeroth order, the expansion is given as [11]

$$\langle J_a^\mu \rangle_{(0)} = n_a u^\mu, \tag{2.7}$$

$$\langle T^{\mu\nu} \rangle_{(0)} = \epsilon u^\mu u^\nu + p\Delta^{\mu\nu}, \tag{2.8}$$

where ϵ is identified as the energy density, p as the equilibrium pressure and n_a as the equilibrium charge density. In ideal hydrodynamics, these quantities are then promoted to slowly varying fields. Now, $\epsilon(x)$ is defined as the local energy density, $p(x)$ as the local pressure and $n_a(x)$ as the local charge density. These functions can then be expressed in terms of $T(x)$, $\mu_V(x)$ using the usual thermodynamic relations from the free energy, F defined at equilibrium.

At first order, one has to deal with a large set of ambiguities as redefinitions of local temperature, chemical potential and fluid velocity compete with terms at higher order in the derivatives. This stems from the fact that $T(x)$, $\mu_V(x)$ and $u^\mu(x)$ have no first-principles definition out of equilibrium and should be thought as nothing more than auxiliary parameters in terms of which the relevant currents are given. The ambiguity issue is resolved by specifying a frame

[1] One should consult [12] regarding contribions from second order terms

choice. In this case, we first choose the Landau frame [13]. This frame is defined by demanding $T^{\mu\nu}u_\nu = \epsilon u^\mu$ to all orders, implying that $q = 0$ in (2.4). Before proceeding, as we want to study anomalies in the microscopic theory, we turn on the sources defined as the electric, magnetic fields in the local rest frame along with the local vorticity

$$B_a^\nu = \frac{1}{2}\epsilon^{\mu\nu\rho\sigma}u_\mu F_{\rho\sigma a}, \tag{2.9}$$

$$E_a^\mu = F_a^{\mu\nu}u_\nu, \tag{2.10}$$

$$\omega^\nu = \frac{1}{2}\epsilon^{\mu\nu\rho\sigma}u_\mu\partial_\rho u_\sigma, \tag{2.11}$$

which will act as sources for various kinds of anomalous response, as we will see. Leaving out the details of the derivation [11], it turns out that at first order, the constitutive relations are

$$\langle J_a^\mu\rangle_{(1)} = -\gamma_{ab}T\Delta^{\mu\nu}\partial_\nu\Big(\frac{\mu_b}{T}\Big) + \gamma_{ab}E_b^\mu + \xi_{ab}^B B_b^\mu + \xi_{a\Omega}\omega^\mu, \tag{2.12}$$

$$\begin{aligned}\langle T^{\mu\nu}\rangle_{(1)} = &-\eta\Delta^{\mu\rho}\Delta^{\nu\sigma}\Big(\partial_\rho u_\sigma + \partial_\sigma u_\rho - \frac{2}{3}\eta_{\rho\sigma}\partial_\lambda u^\lambda\Big)\\ &- \zeta\Delta^{\rho\sigma}\partial_\lambda u^\lambda.\end{aligned} \tag{2.13}$$

The dissipative transport coefficients γ_{ab}, η and ζ are identified as the electric conductivity, shear viscosity and the bulk viscosity respectively. Futhermore, the non-dissipative transport coefficients ξ_{ab}^B and $\xi_{a\Omega}$ are identified as the anomalous conductivities. We will now explain how one comes to the conclusion of this identification [12]. Notice that the spatial components of the $U(1)$ currents, $\langle J_a^i\rangle$ are $\mathcal{P}$-odd, $\mathcal{T}$-odd, while both of the magnetic fields and vorticity are $\mathcal{P}$-even and $\mathcal{T}$-odd. We can then conclude that ξ_{ab}^B, $\xi_{a\Omega}$ are $\mathcal{P}$-odd and $\mathcal{T}$-even. A similar analysis of the other transport coefficients η, ζ and γ_{ab} shows that they are $\mathcal{P}$-even and $\mathcal{T}$-odd. The $\mathcal{T}$-odd coefficients will contribute to entropy production and are thus dissipative in nature. Conversely, the $\mathcal{T}$-even coefficients will not contribute entropy production and are non-dissipative. Considering their microscopic origin, we refer to these non-dissipative conductivities as anomalous conductivities from now on.

2.2 Anomalous Transport in Hydrodynamics

When computing anomalous conductivities, it makes more sense to present the constitutive relations in the no-drag frame [14]; contributions to the energy current in the Landau frame are not directly visible because they are absorbed into the definition of the fluid velocity. In the no-drag frame, the currents read

$$\langle J_a^\mu\rangle = \langle J_a^\mu\rangle_{(0)} - \gamma_{ab}T\Delta^{\mu\nu}\partial_\nu\Big(\frac{\mu_b}{T}\Big) + \gamma_{ab}E_b^\mu + \sigma_{ab}^B B_b^\mu + \sigma_{a\Omega}\omega^\mu, \tag{2.14}$$

$$\langle T^{\mu\nu}\rangle = \langle T^{\mu\nu}\rangle_{(0)} + \langle T^{\mu\nu}\rangle_{(1)} + \mathcal{Q}^\mu u^\nu + \mathcal{Q}^\nu u^\mu, \tag{2.15}$$

where $\mathcal{Q}^\mu = \tilde{\sigma}_a^B B_a^\mu + \tilde{\sigma}_\Omega \omega^\mu$. In the no-frag frame, the fluid velocity only parameterizes the dissipative "normal flow". Physically, if one inserts a heavy impurity into the flow then over long time scales, all of the normal flow will vanish, leaving only the charge and momentum flow induced by the anomalies. The anomalous terms from the above expressions can be identified as the response functions, which we originally wanted to extract from the hydrodynamic setup. Explicitly, they are given as

$$\langle \delta J_a^\mu \rangle = \sigma_{ab}^B B_b^\mu + \sigma_{a\Omega} \omega^\mu \tag{2.16}$$

$$\langle \delta T^{\mu\nu} \rangle = \mathcal{Q}^\mu u^\nu + \mathcal{Q}^\nu u^\mu. \tag{2.17}$$

From this point onwards, we only focus on the U(1) response, dropping the B superscript in (2.16). The Kubo formulae for calculating the conductivities are [7]

$$\sigma_{ab} = \lim_{k\to 0} \epsilon_{ijk} \frac{ik^j}{2k^2} \langle J_a^i J_b^k \rangle \Big|_{\omega=0}, \tag{2.18}$$

$$\sigma_{a\Omega} = \lim_{k\to 0} \epsilon_{ijk} \frac{ik^j}{2k^2} \langle J_a^i T^{tk} \rangle \Big|_{\omega=0}, \tag{2.19}$$

which can be calculated through the use of holographic methods. In this thesis, we will only calculate $\langle \delta J_V^\mu \rangle$. Therefore we will only be concerned with $\sigma_{VV}, \sigma_{AV} = \sigma_{VA}$ and $\sigma_{V\Omega}$, which are associated with the Chiral Magnetic Effect (CME) [5], the Chiral Magnetic Separation Effect (CSE) [15] and the Chiral Vortical Effect (CVE) [16] respectively. The conductivity $\sigma_{A\Omega}$ is associated with the Chiral Vortical Separation Effect (CVSE) whereas σ_{AA} has a different interpretation from the rest of the conductivities [7]. While the axial magnetic field B_A^μ is not expected to exist in nature, it is seen as a tool to compute σ_{VA}, given that from a holographic perspective, $\delta\langle J_V^\mu \rangle$ will be easier to calculate than $\delta\langle J_A^\mu \rangle$. It is for this reason that we do not consider σ_{AA} as it couples to B_A^μ in the $\delta\langle J_A^\mu \rangle$ equation.

It is interesting to note that for the above setup, through the use of hydrodynamcs alone one can almost completely determine the chiral magnetic and chiral vortical conductivities [17]. This is done by defining a local entropy current and demanding it to be positive definite. Such a computation results in the values of the conductivities

$$\sigma_{VV} = \frac{\mu_A}{2\pi^2} \quad , \quad \sigma_{VA} = \frac{\mu_V}{2\pi^2} \quad , \quad \sigma_{V\Omega} = \frac{\mu_V \mu_A}{2\pi^2}. \tag{2.20}$$

These values have been found using multiple approaches, namely an energy balance argument, [18], holography [19], effective field theory [20] and hydrodynamics as we have seen above. This hints at the idea of universality, which has been shown in more formal manner using holography [21], [22]. In the case where dynamical gluons are present, the chiral magnetic and vortical conductivities are expected to deviate from their universal values [23]. This is also clear

from the fact that the universal values (2.20) disagree with lattice QCD calculations [24], which clearly include radiative corrections from such dynamical gluons. The main goal of this thesis will be to calculate such radiative corrections holographically, using a slightly different holographic setup in comparison to [25].

Chapter 3

Chiral Anomalies and Anomalous Transport

Throughout the field of physics, symmetry plays a central role due to the consequence of Noether's Theorem. It often happens that, following the quantization of a theory, some of its symmetries at the classical level do not survive or become anomalous, signifying the presence of a quantum anomaly. In particular, the vanishing of a chiral symmetry at the quantum level is known as a chiral anomaly. While the anomaly might not necessarily be detrimental to the quantum theory's validity, one finds at the very least that the related Ward identities need to be modified.

3.1 The Source of the Anomaly

Computing the Jacobian

Even though anomalies were first observed through the computation of triangle diagrams [26], we will see how they emerge in a more explicit fashion by studying the path integral Jacobian related to chiral transformations [27]. To start, consider the Lagrangian in flat space with massless Dirac spinors transforming under an $SU(N_c)$ gauge group

$$\begin{aligned}\mathcal{L} &= \bar{\psi} i \not{D} \psi - \frac{1}{2g_{\mathrm{YM}}^2} \mathrm{Tr}\big(G_{\mu\nu} G^{\mu\nu}\big), \\ &= \mathcal{L}_{\mathrm{matter}} + \mathcal{L}_{\mathrm{gauge}}. \end{aligned} \tag{3.1}$$

where

$$D_\mu = \partial_\mu - i W_\mu, \tag{3.2}$$

$W_\mu = W_\mu^a t^a$ is the Lie algebra-valued gluon field in the adjoint representation and ψ represents an array of N_f quark fields. As we are only concerned with

exposing the anomaly, for the moment we restrict ourselves to the calculation of how the quantity

$$\int \mathcal{D}\bar{\psi}\mathcal{D}\psi \exp\left[-i\int d^4x \mathcal{L}_{\text{matter}}\right] \tag{3.3}$$

transforms under a chiral transformation. In particular, we write

$$\mathcal{D}\bar{\psi}'\mathcal{D}\psi' = J\mathcal{D}\bar{\psi}\mathcal{D}\psi \tag{3.4}$$

and compute the Jacobian, J. Let us do this explicitly for a chiral transformation

$$\psi' = U\psi \quad , \quad U(x) = \exp\left[i\beta(x)\gamma_5\right] \tag{3.5}$$

Under (3.5), the transformation of the measure appears as a functional determinant,

$$\mathcal{D}\psi \to \mathcal{D}\psi' = (\text{Det}\mathcal{U})^{-1}\mathcal{D}\psi \quad , \quad \mathcal{D}\bar{\psi} \to \mathcal{D}\bar{\psi}' = (\text{Det}\bar{\mathcal{U}})^{-1}\mathcal{D}\bar{\psi}, \tag{3.6}$$

where

$$\langle x|\,\mathcal{U}\,|y\rangle = U(x)\delta^4(x-y) \quad , \quad \langle x|\,\bar{\mathcal{U}}\,|y\rangle = \bar{U}(x)\delta^4(x-y). \tag{3.7}$$

To detect the presence of an anomaly, we must now compute

$$\bar{U}(x) = i\gamma^0 \exp[-i\beta\gamma_5]i\gamma^0 = \exp[i\beta\gamma_5] = U(x). \tag{3.8}$$

This implies that the Jacobian is

$$J = (\text{Det}\mathcal{U})^{-2}, \tag{3.9}$$

which does not necessarily equal unity. The method for computing J is sketched below, where we refer to [28], [29] for further details. The general idea is to expand the spinors in terms of the eigenfunctions of $\not{D}$

$$\not{D}\varphi_n(x) = \lambda_n\varphi_n(x),$$

where

$$\int d^4x \varphi_n^\dagger(x)\varphi_m(x) = \delta_{n,m}, \tag{3.10}$$

which allows us to express the determinant in a gauge-invariant way. One realizes that this is necessary—if ψ transforms in a covariant way then so should $\mathcal{D}\psi$. It turns out that the Jacobian takes the form

$$J = \exp\left[-2i \lim_{N\to\infty}\sum_{n=1}^{N}\int d^4x\beta\,\text{Tr}\Big(\varphi_n^\dagger\gamma_5\varphi_n\Big)\right]. \tag{3.11}$$

Hidden within the argument of the exponential is a $\delta(0)$, which implies that we should introduce a regulator, $f(s)$. Such a regulator effectively cuts off the "high

frequency" modes, the large eigenvalues of $\not{D}$ and is manifestly gauge-invariant. The regulator is introduced by writing

$$\begin{aligned}
&\lim_{N\to\infty}\sum_{n=1}^{N}\int d^4x\beta\,\mathrm{Tr}\Big(\varphi_n^\dagger\gamma_5\varphi_n\Big)\\
&=\lim_{M\to\infty}\sum_{n=1}^{\infty}\int d^4x\beta\,\mathrm{Tr}\left(\varphi_n^\dagger\gamma_5 f\Big(\frac{\lambda_n^2}{M^2}\Big)\varphi_n(x)\right)\\
&=\lim_{M\to\infty}\sum_{n=1}^{\infty}\int d^4x\beta\,\mathrm{Tr}\left(\varphi_n^\dagger\gamma_5 f\Big(\frac{\not{D}^2}{M^2}\Big)\varphi_n(x)\right),
\end{aligned}\tag{3.12}$$

where $f(s)$ is an arbitrary smooth function such that

$$f(0)=1\quad,\quad f(\infty)=0\quad,\quad sf'(s)|_{s=0}=0\quad,\quad sf'(s)|_{s=\infty}=0.\tag{3.13}$$

The calculation of this quantity is quite a lengthy procedure, which can be found in [28]. The final result is

$$\begin{aligned}
J&=\exp\big[-2i\int d^4x\frac{1}{32\pi^2}\beta\epsilon^{\mu\nu\rho\sigma}\,\mathrm{Tr}\big(G_{\mu\nu}G_{\rho\sigma}\big)\big],\\
&=\exp\Big[i\int d^4x\beta\mathcal{A}_1\Big],
\end{aligned}\tag{3.14}$$

where we have defined the anomaly function

$$\mathcal{A}_1=-\frac{N_f}{16\pi^2}\epsilon^{\mu\nu\rho\sigma}\,\mathrm{Tr}\big(G_{\mu\nu}G_{\rho\sigma}\big)\tag{3.15}$$

and $G_{\mu\nu}=\partial_\mu W_\nu-\partial_\nu W_\mu$, the gluon field strength tensor.

By restoring factors of $\hbar$ through a redefinition of the action $S\to S/\hbar$, one can see that J actually corresponds to a one-loop effect. It is then natural to wonder if the anomaly equation (3.14) recieves any corrections when diagrams with more than one loop are taken into account. It was shown by Adler and Bardeen using a diagrammatic approach [30] that this is not the case, implying that the anomaly is one-loop exact. We note that this is a major argument for identifying the anomaly with the non-invariance of the path integral measure.

Atiyah-Singer Index Theorem

One can also invoke the Atiyah-Singer index theorem [31] to strengthen this argument, as we will now see. Even though the proof was initially demonstrated for a Dirac operator on S^4, we will present its adaption to our situation. Specializing to the case where a global transformation is parameterized by $\beta(x)=\beta$ with a single quark flavor, we sketch the proof for the analytical index of the

hermitean operator $i\not{D}^E$, where $\not{D}^E$ is a Euclidean operator. Recalling (3.10), and using the fact that $\{i\not{D}^E, \gamma_5\} = 0$ by definition, we can show that for $\lambda_n^E \neq 0$

$$i\not{D}^E(\gamma_5\varphi_n) = -\lambda_n^E\gamma_5\varphi_n, \tag{3.16}$$

which implies that φ_n and $\gamma_5\varphi_n$ are orthogonal functions. Hence, eigenfunctions of the non-zero eigenvalues will not contribute to the argument of the exponential in (3.11).

Let us now specialize to the case where $\lambda_n^E = 0$. For these zero modes, we can simultaneously diagonalize $i\not{D}^E$ and γ_5 because both $\varphi_n, \gamma_5\varphi_n$ have the same eigenvalue, namely zero. These eigenfunctions clearly will contribute to (3.11). In fact, the total contribution will read

$$\int d^4x \sum_{\text{zero modes}} \varphi_n^\dagger\gamma_5\varphi_n = \text{index}(i\not{D}^E) \tag{3.17}$$

where $\text{index}(i\not{D}^E) = n_L - n_R$ and n_L, n_R are respectively the number of $+1, -1$ eigenvalues of the matrix γ_5. Using the results of the previous section, we can write

$$\text{index}(i\not{D}^E) = \frac{1}{32\pi^2}\int d^4x\epsilon^{\mu\nu\rho\sigma}\,\text{Tr}\big(G_{\mu\nu}G_{\rho\sigma}\big). \tag{3.18}$$

Obviously, the left hand side is an integer. The right hand side is also an integer — this is known as the winding number and it reveals the topological class to whch the field W^μ belongs. We explicitly relate this to the Jacobian by writing

$$J = \exp\left[i\beta\int d^4x\mathcal{A}_1(x)\right] = \exp\big[-2i\beta(n_L - n_R)\big]. \tag{3.19}$$

Now that we have sufficiently demonstrated where the origin of the anomaly lies, we can go on and exhibit how one modifies the relevant Ward identities.

3.2 Modification of Ward Identities

We now present the full theory of interest, which we will later on attempt to model using holography. We have included external vector and axial gauge fields, which are denoted by the flavor singlets, V_μ and A_μ respectively. The action is

$$S = \int d^4x\bar{\psi}\not{D}\psi - \frac{1}{2g_{\text{YM}}^2}\,\text{Tr}\big(G_{\mu\nu}G^{\mu\nu}\big) - \frac{N_f}{16\pi^2}\theta\epsilon^{\mu\nu\rho\sigma}\,\text{Tr}\big(G_{\mu\nu}G_{\rho\sigma}\big), \tag{3.20}$$

where the last term is CP-odd and includes the topological effects of such non-abelian gauge theories[1]. The covariant derivative is further modified because of

[1]This term is directly related to the winding number mentioned in (3.18).

the background gauge fields

$$D_\mu = \partial_\mu - i(W_\mu + q_f V_\mu + \gamma^5 A_\mu). \tag{3.21}$$

The coupling constants q_f are different for each of the quark flavors, meaning that we assume implicit multiplication in flavor space. At the classical level, the action 3.20 is invariant under the group of chiral transformations $U(N_f)_L \times U(N_f)_R$, which we rewrite as $U(1)_V \times U(1)_A \times SU(N_f)_L \times SU(N_f)_R$. The action of each subgroup on the quark fields is

$$\psi_L \to e^{i\alpha}\psi_L \quad , \quad \psi_R \to e^{i\alpha}\psi_R, \tag{3.22}$$

$$\psi_L \to e^{i\beta}\psi_L \quad , \quad \psi_R \to e^{-i\beta}\psi_R, \tag{3.23}$$

$$\psi_L \to U_L\psi_L \quad , \quad \psi_R \to U_R\psi_R, \tag{3.24}$$

where the left and right-handed components of the spinors have been defined with the use of the usual projectors [1]

$$P_L = \frac{1-\gamma^5}{2} \quad , \quad P_R = \frac{1+\gamma^5}{2} \tag{3.25}$$

where we again assume multiplication in flavor space. The vector and axial phase transformations are determined by α and β respectively[2] while U_L, U_R are the $SU(N_f)_{L/R}$ matrices.

The full symmetry group is drastically affected by the quantization of the theory. While it is not relevent for our discussion, the existence of the quark condensate in the QCD vacuum induces the spontaneous symmetry breaking $SU(N_f)_L \times SU(N_f)_R \to SU(N_f)_V$ where $SU(N_f)_V$ is the diagonal subgroup of $SU(N_f)_L \times SU(N_f)_R$. This mechanism is thought to be responsible for the observed spectrum of pions observed in particle physics experiments[3]. Only the $U(1)_V$ subgroup remains untouched. As we will see shortly, its associated Noether current

$$\mathcal{J}^\mu_V = iq_f\bar{\psi}\gamma^\mu\psi \tag{3.26}$$

is conserved on an operator level signifying the conservation of electric charge. The classical axial Noether current is

$$\mathcal{J}^\mu_A = i\bar{\psi}\gamma^\mu\gamma_5\psi. \tag{3.27}$$

As we observed in the previous section, this symmetry becomes anomalous as a consequence of the quark path integral measure's transformation properties. We will now see how the related Ward identity is affected. Let us only consider

[2] This is in keeping with the notation (3.5) used in the previous section.

[3] In reality pions are not massless, which they should be according to Goldstone's theorem. This is due to the fact that the chiral symmetry is only approximate after quark mass terms are added to the theory by hand.

the matter part, $S_{\rm matter}[\bar\psi,\psi]=\int d^4x\bar\psi\not{D}\psi$ of the (3.20) and observe the change of the quark fields under vector and axial phase transformations

$$\begin{aligned}\int\mathcal{D}\bar\psi\mathcal{D}\psi e^{iS_{\rm matter}[\bar\psi,\psi]}&=\int\mathcal{D}\bar\psi'\mathcal{D}\psi' e^{iS_{\rm matter}[\bar\psi',\psi']}\\&=\int\mathcal{D}\bar\psi\mathcal{D}\psi J e^{iS_{\rm matter}[\bar\psi,\psi]+i\int d^4x(\alpha\partial_\mu\mathcal{J}^\mu_V+\beta\partial_\mu\mathcal{J}^\mu_A)}.\end{aligned}\tag{3.28}$$

Our definition of J needs to be modified to take into account the additional anomaly functions that arise due to the inclusion of the external fields V_μ, A_μ. Similar to the calculation outlined in the previous section, one can show that [28]

$$\mathcal{A}_2=-\frac{N_f}{32\pi^2}\sum_{f=1}^{N_f}q_f^2\epsilon^{\mu\nu\rho\sigma}F^V_{\mu\nu}F^V_{\rho\sigma},\tag{3.29}$$

$$\mathcal{A}_3=-\frac{N_cN_f}{96\pi^2}\epsilon^{\mu\nu\rho\sigma}F^A_{\mu\nu}F^A_{\rho\sigma}.\tag{3.30}$$

The full Jacobian is then

$$J=\exp\Big[i\int d^4x\beta\mathcal{A}\Big],\tag{3.31}$$

where $\mathcal{A}=\mathcal{A}_1+\mathcal{A}_2+\mathcal{A}_3$. Expanding (3.28) up to first order in α,β yields

$$\begin{aligned}\int\mathcal{D}\bar\psi\mathcal{D}\psi e^{iS_{\rm matter}[\bar\psi,\psi]}=\int\mathcal{D}\bar\psi\mathcal{D}\psi e^{iS_{\rm matter}[\bar\psi,\psi]}\Big(1\\+i\int d^4x(\alpha\partial_\mu\mathcal{J}^\mu_V+\beta(\mathcal{A}(x)+\partial_\mu\mathcal{J}^\mu_A)\Big).\end{aligned}\tag{3.32}$$

As α,β are independent we can immediately read off the Ward identities

$$\partial_\mu\langle\mathcal{J}^\mu_V\rangle=0,\tag{3.33}$$

$$\partial_\mu\langle\mathcal{J}^\mu_A\rangle=-\mathcal{A}.\tag{3.34}$$

Indeed, the axial equation above is an example of an anomalous Ward identity. There is a subtlety that we have glossed over with repsect to the presentation of the identities above [32]. In particular, the expressions are defined as the consistent currents and are constructed in such a way that the vector current is conserved[4]. Depending on the physical situation that one is intending to describe, it may be preferable to construct a current that is invariant under gauge transformations. With this in mind, one can define a covariant current by adding the Bardeen-Zumino polynomial [32] to the previously defined consistent currents

$$J^\mu_V=\mathcal{J}^\mu_V+\frac{N_cN_f}{4\pi^2}\epsilon^{\mu\nu\rho\sigma}A_\nu F^V_{\rho\sigma},\tag{3.35}$$

$$J^\mu_A=\mathcal{J}^\mu_A+\frac{N_cN_f}{12\pi^2}\epsilon^{\mu\nu\rho\sigma}A_\nu F^A_{\rho\sigma}.\tag{3.36}$$

[4]More formally, such a prescription ensures that the Wess-Zumino consistency condition is satisfied.

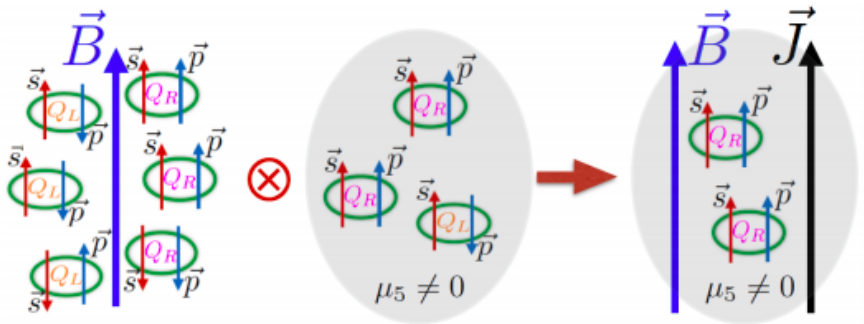

Figure 3.1: Illustration of the Chiral Magnetic effect, taken from [33].

3.3 Anomalous Transport in High Energy Physics

We have seen how quantum anomalies emerge through the consideraton of the path integral under chiral transformations. It is then natural to wonder if these phenomena could possibly manifest themselves on a macroscopic level, specifically in the context of high energy physics. The presence of non-zero chiral imbalance, μ_A alone is a necessary but not sufficient ingredient needed to produce macroscopically observable anomalous effects. We also need the presence of a chiral medium, which in this case is given by an external magnetic field $\vec{B}$, at least for the CME and CSE. Below we will attempt to paint a qualitative picture arguing how such manifestations could arise, following [2] and [33]. Although we only specify the dependence of anomalous response currents below, it should be emphasized that each of the conductivities have been found to take their universal values (2.20) in the absence of dynamical gluons, as was discussed at the end of the last Chapter 2.

The Chiral Magnetic Effect

Consider the QGP, which in this context can be regarded as a conductor with deconfined electrically charged quarks[5]. For simplicity, we only consider one quark flavor. As is depicted in the left part of 3.1, the application of an external magnetic field leads to a magnetization effect with the quarks' spins, $\vec{s}$ aligned along the direction of $\vec{B}$. Specifically, the right-handed quarks will have $\vec{p}||\vec{s}$ and the left-handed quarks will have $\vec{p}||-\vec{s}$, where $\vec{p}$ is the quark's momentum. Furthermore, if a chiral imbalance, $\mu_A > 0$ is introduced, the chirality of the left-handed quarks will flip, inducing an electric current, $\vec{J} \propto \mu_A \vec{B}$. This shown

[5]We are speaking of massless quarks, which means that the projection of spin onto momentum, also known as helicity is equivalent to the notion of chirality.

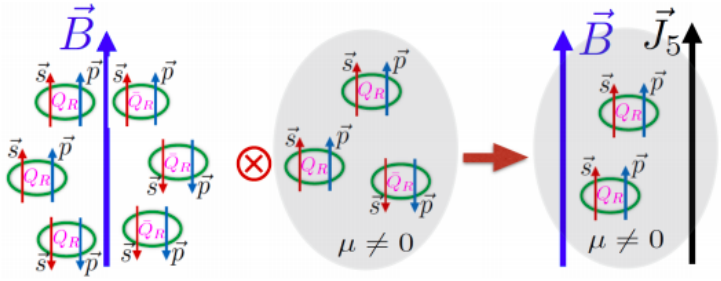

Figure 3.2: Illustration of the Chiral Separation Effect, taken from [33].

in the right of Fig 3.1.

The Chiral Separation Effect

It is then natural to wonder if an axial current, $\vec{J}_A$ could be produced using a similar setup. The answer is yes, at least theoretically. Here we start by considering sea of right-handed quarks. Again, we only consider a single flavor for simplicity. As is shown in the left of Fig 3.2, the application of a magnetic field induces a magnetization of the quark's spins. The essence of the CSE is contained within the fact that we then turn on a non-zero vector chemical potential, $\mu_V > 0$. The right-handed quarks will then generate a current $\vec{J}_R \propto \mu_V \vec{B}$. Similarly, the left handed quarks will form a current in the opposite direction $\vec{J}_L \propto mu\vec{B}$. The combination of the two yields the axial current[6], $\vec{J}_A \propto \mu\vec{B}$. The interpretation of the CSE is that it is simply the CME for purely left-handed or right-handed quarks.

The Chiral Vortical Effect

It is also possible for anomalous transport effects to take place when a fluid of chiral fermions undergoes a global rotation. This is introduced by defining a vorticity, $\vec{\omega} = \frac{1}{2}\vec{\nabla} \times \vec{v}$ where $\vec{v}$ is the flow velocity field. As is shown in the left of Fig 3.3, in the presence of a global rotation, the quarks experience an effective interation $\sim -\vec{\omega} \cdot \vec{s}$. This induces a spin polarization effect, similar to the case of the CME and CSE. The difference here is that the polarization effect is charge-blind, in comparison to the magnetization, which is needed for the CME and CSE to occur.

Two further ingredients necessary for the CVE is a non-zero μ_V, μ_A. Given $\mu_A > 0$, there will be more right-handed quarks than left-handed quarks and

[6]The author of the paper [18] with Fig 3.2 writes this current as $\vec{J}_5$.

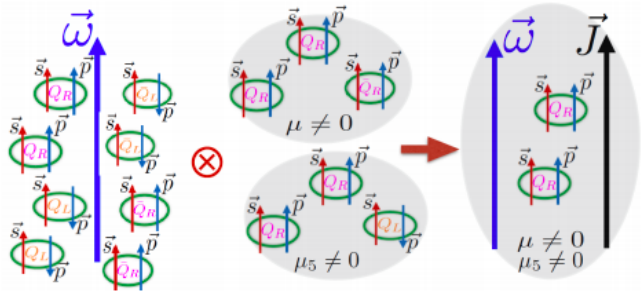

Figure 3.3: Illustration of the Chiral Vortical Effect, taken from [33].

given $\mu_V > 0$, there will be more right-handed quarks than right-handed anti-quarks. The combination leads to the generation of a current $\vec{J} \propto \mu_V \mu_A \vec{\omega}$. The inclusion of the factor $\mu_V \mu_A$ comes from the fact that if either μ_V or μ_A equals zero, the current will cease to exist owing to cancellations.

Chapter 4

Holographic Applications to QCD

Holography is intuitively understood as an attempt to geometrize the renormalization group flow in quantum field theories (QFT) or more generally, many-body systems. Specifically, this should be done by first considering a continuous family of D-dimensional theories, each labelled by some length scale[1] r. The length scale is then identified with an extra spatial dimension, yielding a single $D+1$-dimensional theory. Among the requirements of such an identification is that the D-dimensional and $D+1$-dimensional theories should have the same number of degrees of freedom.

In general, it is not known how to construct this mapping between theories. However, some guidance is provided by the fact that the $D+1$-dimensional theory may be a description of quantum gravity, which is suggested by the holographic principle— the holographic principle [34] asserts that for a gravitational theory, the number of degrees of freedom in a volume V scales with the boundary of the volume itself, ∂V. The AdS/CFT correspondence proposed by Maldecena [35] in 1997 is an explicit realisation of this idea. We will briefly motivate why this is so, following [36] before providing a more concrete summary of the topic.

As our D-dimensional quantum field theory lives in Minkowski space, we present the most general metric in $D+1$ dimensions consistent with D-dimensional Poincaré symmetry

$$ds^2 = \Omega^2(r)(-dt^2 + d\vec{x}^2 + dr^2). \tag{4.1}$$

The warp factor Ω can only depend on r as we demand translational invarance in the other space and time directions. Let us now specialize to the case where our

[1] We follow the convention where $r \to 0$ limit is identified with the UV limit of the QFT while the $r \to \infty$ limit is identified with the IR limit of the QFT.

quantum field theory possesses conformal symmetry. A conformal field theory (CFT) is invariant under the transformation $(t, \vec{x}) \to C(t, \vec{x})$ for a constant C. As r represents the length scale in our CFT, our gravity theory should have $r \to Cr$ fixing

$$\Omega(r) = \frac{L}{r}, \tag{4.2}$$

where L is some constant. We then proceed to identify L with the anti-de Sitter (AdS) radius, precisely because

$$ds^2 = \frac{L^2}{r^2}(-dt^2 + d\vec{x}^2 + dr^2) \tag{4.3}$$

is the metric for AdS spacetime in $D+1$ dimensions. It is not hard to see that each constant r-slice of this spacetime is isometric to some D-dimensional theory living in Minkowski space with coordinates $(t, \vec{x})$. In particular, if we take the limit $r \to 0$, we recover the conformal field theory itself[36]. This is why it is often said that the CFT "lives on the boundary" of AdS.

4.1 The AdS/CFT Correspondence

Maldacena's original conjecture is motivated by considering type IIB superstring theory in $(9+1)$-dimensional Minkowski spacetime from the perspective of both open and closed strings. For practical applications it is necessary to take the so-called weak form of the duality. This is done by comparing both perspectives in the low-energy limit, where one concludes that there should exist an equivalence between $\mathcal{N} = 4$ super Yang-Mills (sYM) in $3+1$ dimensional flat space and type IIB classical supergravity on $AdS_5 \times S_5$ given that the free parameters of each theory are identified in the way described below.

The parameters on the field theory side are g_{YM}, the Yang-Mills coupling and N, the rank of the gauge group while on the string theory side they are g_{s}, the string coupling and the ratio L^2/α' where L is the radius of curvature and $\alpha' = l_{\mathrm{s}}^2$ with l_{s} the string length [37]. The correspondence is established by the identification

$$g_{\mathrm{YM}}^2 = 2\pi g_{\mathrm{s}} \quad , \quad 2g_{\mathrm{YM}}^2 N = \frac{L^4}{\alpha'^2} \tag{4.4}$$

where we also note that the 't Hooft coupling is $\lambda = g_{\mathrm{YM}}^2 N$. The weak form of the duality then corresponds to taking the 't Hooft limit where $N \to \infty$ and also demanding $\lambda \gg 1$. On the string theory side, if $g_{\mathrm{s}} \to 0$ then from the perspective of perturbative string theory, we are only including tree level diagrams while $\alpha'/L^2 \to 0$ amounts to the point-particle limit.

The AdS/CFT correspondences proposes a map between two different theories [38]. The one-to-one map or dictionary is a consequence of the fact that the symmetry groups of the two theories coincide. Such a mapping is known as the field-operator map and is made more explicit by considering the boundary

behaviour of the supergravity fields. We therefore consider this behaviour for a free scalar field, ϕ in $D+1$ dimensions with the action

$$S = -\frac{Y}{2}\int dr d^D x\sqrt{-g}\Big(g^{MN}\partial_M\phi\partial_N\phi + m^2\phi^2\Big), \tag{4.5}$$

where g is defined according to (4.3). From here onwards, we will denote the bulk theory's tensor indices by the latin letters $M, N, ...$ while as usual the QFT's indices will be denoted by the Greek letters $\mu, \nu, ...$ One finds that after comptuting the associated equation of motion for the scalar field and performing the Fourier decomposition $\phi(r,x) = e^{ip^\mu x_\mu}\phi_p(r)$, the Klein-Gordon equation for the modes $\phi_p(r)$ reads

$$r^2\partial_r^2\phi_r(z) - (D-1)r\partial_r\phi_p(r) - (m^2L^2 + p^2r^2)\phi_p(r) = 0. \tag{4.6}$$

Asymptotically, there exist two independent solutions

$$\lim_{r\to 0}\phi_p(r) \sim \begin{cases} r^{\Delta_+} & \text{normalizable,} \\ r^{\Delta_-} & \text{non-normalizable,} \end{cases}$$

where

$$\Delta_\pm = \frac{D}{2} \pm \sqrt{\frac{D^2}{4} + m^2L^2} \tag{4.7}$$

A mode is normalizable if the action evaluated on this solution is finite. Moreover, if we write

$$\phi(r,x) \sim \phi_0(x)r^{\Delta_-} + \phi_+(x)r^{\Delta_-} + ..., \tag{4.8}$$

where

$$\phi_0(x) = \lim_{r\to 0}\phi(r,x)r^{-\Delta_-} \quad , \quad \phi_+(x) = \lim_{r\to 0}\phi(r,x)r^{-\Delta_+} \tag{4.9}$$

and ... represents the subleading terms at the boundary. One can then conclude via dimensional analysis that the normalizable mode corresponds to the vacuum expectation value for a dual scalar field theory operator $\mathcal{O}$ with conformal dimension Δ_+. Conversely, ϕ_0 is identified as the source of such an operator.

Having seen how the field-operator map works for a scalar field, we will now observe in general how it induces a map between the genererating functionals of both theories. In Euclidean signature, for a D-dimensional conformal theory living on the boundary of $(D+1)$-dimensional AdS space, this is stated as

$$Z_{\text{string}}\Big|_{\lim_{r\to 0}\phi(r,x)r^{\Delta_- - D} = \phi_0(x)} = \left\langle \exp\Big(\int d^D x\phi_0(x)\mathcal{O}(x)\Big)\right\rangle_{\text{CFT}} \tag{4.10}$$

for a scalar field $\phi(x)$. This holds for the strongest form of the correspondence, where Z_{string} is not necessarily known. Assuming the weak form of the correspondence, we may perform a saddle point approximation on the string partition

function and conclude that

$$\exp\Big(-S_{\text{Sugra}}[\phi]\Big)\Big|_{\lim_{r\to 0}\phi(r,x)r^{\Delta--D}=\phi_0(x)} = \Big\langle \exp\Big(\int d^D x\phi_0(x)\mathcal{O}(x)\Big)\Big\rangle_{\text{CFT}}$$
$$= \exp\Big(-W[\phi_0]\Big) \tag{4.11}$$

where S_{Sugra} is the on-shell bulk action, which acts as the generating functional, $W[\phi_0]$ for connected correlation functions involving the operator $\mathcal{O}(x)$. The usefulness of the duality is now made manifest through the fact that we can compute these connected correlation functions by functional differentiation with respect to the sources

$$-\frac{\delta^n W[\phi_0(x)]}{\delta\phi_0^1(x_1)\delta\phi_0^2(x_2)...\delta\phi_0^n(x_n)}\Big|_{\phi_0^i=0} = \Big\langle \mathcal{O}_1(x_1)\mathcal{O}_2(x_2)...\mathcal{O}_n(x_n)\Big\rangle_{\text{CFT}}. \tag{4.12}$$

Having demonstrated the power of this approach for a scalar operator, it is important to note that one can do the same for other gauge invariant operators on the boundary theory after identifying, respectively, their dual fields on the gravity side 37. Some of these results are summarized in Table 4.1.

At this point we should probably mention how the extra five dimensions of S_5 affect the establishment of the duality [39]. Arising from the compactification of S_5 is the emergence of Kaluza-Klein (KK) modes. This results in the existence of an additional sector in the bulk Hilbert space. Fortunately, the operators spanning this sector turn out to be in precise correspondence with the operators with higher conformal dimension on the field theory side. When the low-energy limit is taken, the subsector of the Hilbert space containing $\mathcal{N}=4$ super-multiplets of the energy-momentum tensor and flavor currents can be identified with the low-lying gravitational fields.

While the case described above is the most well understood of the conjecture, progress towards understanding more realistic theories can be obtained from $\mathcal{N}=4$ sYM by relevant or marginal deformations. In particular, attempts to model QCD holographically can be categorized into top-down and bottom-up models. The top-down approach generally consists of starting from some D-brane setup in string theory and taking the decoupling limit to obtain gravitational a background with various form fields [40]. While this has the advantage of providing us with a precise dictionary between the QFT on the D-branes and the dual gravitational quantities, the resultant QFT often turns out to be different from QCD. In addition to this, it is found that in order to decouple the KK modes operators from pure Yang-Mills one needs to take the limit of large curvature on the gravity side, necessitating the inclusion of higher derivative terms in the bulk action. Due to these obstructions, we attempt to study QCD using a bottom-up model in this thesis, namely V-QCD. From this point onwards, as we are attempting to describe a $3+1$-dimensional quantum field theory, we specialize to the case where the bulk theory lives in five spacetime dimensions.

Gravity	QFT
D+1 dimensions	D dimensions
Holographic direction	RG scale
Strongly coupled	Weakly coupled
Scalar field	Scalar operator
Gauge field	Conserved current
Metric tensor	Energy-momentum tensor

Table 4.1: The holographic dictionary, taken from [10].

4.2 V-QCD

The idea of a bottom-up model is to give up the ambitious goal of trying to find an exact holographic dual of QCD, instead attempting to construct an IR effective theory [39]. As was already mentioned, the class of bottom-up models we choose to work with is V-QCD [41]. V-QCD is based on the combination of two frameworks, namely Improved Holographic QCD (IHQCD) [42], which attempts to model the gluonic sector and a setup based on a Sen-like tachyonic Dirac-Born-Infield (DBI) action, which attempts to model the quark sector [43]. Before we proceed to oultine separately the structure of each of these sectors, it is worth mentioning the issue of taking the $N_c \to \infty$. In this limit, the effect of quarks is suppressed by powers of $N_f/N_c \to 0$, which corresponds to the "quenched limit" [44]. In order for the quarks to backreact onto the supergravity background, we should instead take the Veneziano limit [45],

$$N_c \to \infty \quad , \quad N_f \to \infty \quad , \quad \frac{N_f}{N_c} = x, \tag{4.13}$$

where x is fixed. We take $x = 1$ from now on.

Glue Sector

Our task of holographically modelling the gluonic sector of QCD is simplified somewhat by the fact that a sector of relevant and marginal low-lying operators can be treated separately from the rest of the Hilbert space of operators [46]. Therefore, we can start by looking for bulk theory, which is holographically dual to an $SU(N_c)$ gauge theory. This dual model should correspond to some five dimensional non-critical string theory. It is reassuring that if we are only interested in studying the IR physics, we need not worry about our general lack of knowledge about non-critical string theories since we should be able to approximate the holographic dual by a two-derivative gravitational action.

In our model, the only field that we will be concerned with from IHQCD is the dilaton, $\lambda = e^{\Phi}$, which is dual to the scalar gluonic operator, $\mathrm{Tr}\, G_{\mu\nu}G^{\mu\nu}$

and therefore sources the 't Hooft coupling in Yang-Mills theory[2]. In order to use holography, we want the solutions to approach the AdS_5 spacetime near the conformal boundary. However, we do not want the symmetries of AdS to be respected all the way into the interior of the bulk theory, because of the running of the coupling constant in QCD. In particular, we want to break the scaling symmetry. In the bulk theory, this is achieved by writing down a non-trivial potential for the dilaton, $V_g(\lambda)$. Generally, one tries to model these bulk potentials with the ansatz [47]

$$V(\lambda) = \sum_{k=0}^{n_{\rm UV}} V_k \lambda^k + e^{-\tilde{\lambda}_0/\lambda}(\lambda/\tilde{\lambda}_0)^\alpha \log\Big(1+\lambda/\tilde{\lambda}_0\Big)^\beta \sum_{k=0}^{n_{\rm IR}} v_k (\lambda/\tilde{\lambda}_0)^{-k}. \quad (4.14)$$

For the gluonic potential, $V_g(\lambda)$, the coefficients V_1 and V_2 are fixed by requiring the UV RG flow of the 't Hooft coupling to be the same as in QCD up to two-loop order. The IR coefficients are chosen to reproduce qualitative features of QCD such as confinement, magnetic charge screening and linear glueball trajectories through a comparison with lattice data [48]. This results in the choice

$$V_g(\lambda) = 12\left[1+V_1\lambda+\frac{V_2\lambda^2}{1+\lambda/\tilde{\lambda}_0}+V_{\rm IR}e^{-\tilde{\lambda}_0/\lambda}(\lambda/\tilde{\lambda}_0)^{4/3}\sqrt{\log\Big(1+\lambda/\tilde{\lambda}_0\Big)}\right], \quad (4.15)$$

where the explicit values for the coefficients are given in Appendix A. The gluonic part of our action is then based on Einstein-dilaton theory

$$S_g = M_p^3 N_c^2 \int d^5x\sqrt{-g}\left(R - \frac{4}{3}\frac{(\partial_M\lambda)^2}{\lambda^2} + V_g(\lambda)\right), \quad (4.16)$$

where M_p is the Planck mass.

Flavor Sector

Quarks are included in the holographic setup by embedding flavor branes in the 5D geometry [43]. Specifically, these are space-filling N_f D4-branes and N_f $\bar{D}4$-branes. The low-lying fields on the branes are the tachyon, T as well as the gauge-fields, $A_{L,\mu}$ on the flavor branes and $A_{R,\mu}$ on the anti-flavor branes. The tachyon sources the quark mass matrix, while the gauge fields correspond to the flavor currents in QCD. As we are interested in studying the QGP, we turn off the tachyon as the quark condensate is not expected to play a role in this phase of QCD[3]. For future reference, we rewrite the gauge fields in terms

[2]Technically, the field Φ is the dilaton. However, because we will not need to mention Φ at any other point there will be no ambiguity present by referring to λ as the dilaton.

[3]It is expected however, that the inclusion of the tachyon will produce some of the more realistic features of the QCD phase diagram. We will provide a discussion related to this in the Conclusion 7.

of their vector and axial components

$$\begin{aligned} A_{L,M} &= V_M + A_M, \\ A_{R,M} &= V_M - A_M. \end{aligned} \tag{4.17}$$

These are packaged into the action through the effect DBI term

$$S_f = -\frac{xM_p^3 N_c^2}{2} \int d^5x V_f(\lambda) \Big[\sqrt{-\det \boldsymbol{A}_+} + \sqrt{-\det \boldsymbol{A}_-} \Big], \tag{4.18}$$

where

$$\boldsymbol{A}_{(\pm)MN} = g_{MN} + w(\lambda)(F^V_{MN} \pm F^A_{MN}), \tag{4.19}$$

and

$$\begin{aligned} F^V_{MN} &= \partial_M V_N - \partial_N V_M, \\ F^A_{MN} &= \partial_M A_N - \partial_N A_M. \end{aligned} \tag{4.20}$$

The potentials $V_f(\lambda)$ and $w(\lambda)$ are chosen in a similar manner to that of $V_g(\lambda)$, starting from the ansatz (4.14). They are given as

$$V_f(\lambda) = W_0 + W_1\lambda + \frac{W_2\lambda^2}{1+\lambda/\tilde{\lambda}_0} + W_{\rm IR} e^{-\tilde{\lambda}_0/\lambda} (\lambda/\tilde{\lambda}_0)^2, \tag{4.21}$$

$$\frac{1}{w(\lambda)} = w_0 \left[1 + \bar{w}_0 e^{\hat{\lambda}_0/\lambda} \frac{(\lambda/\hat{\lambda}_0)^{4/3}}{\log\Big(1+\lambda/\hat{\lambda}_0\Big)} \right]. \tag{4.22}$$

The UV coefficients of the above two potentials are determined by comparison with QCD beta function while the IR coefficients are chosen to reproduce some of the prominent features of the QCD phase diagram, such as chiral symmetry breaking and linear meson trajectories.

Anomalous Sector

CP-odd effects are taken into account [43] by the addition of the term

$$S_a = -\frac{M_p^3 N_c^2}{2} \int d^5x \sqrt{-g} Z(\lambda) (\partial_M \mathfrak{a} - 2x A_M)^2. \tag{4.23}$$

where the axion, $\mathfrak{a}$ is dual to the term $\epsilon^{\mu\nu\rho\sigma} \operatorname{Tr}\big(G_{\mu\nu} G_{\rho\sigma}\big)$, sourcing the θ-angle. According to [49], the mass term for A_M produced by the above action is necessary to include gluonic contributions to the model of anomalous transport; a massive axial gauge field will source a current $\mathcal{J}_A$ with non-vanishing anomalous dimension. The axion then ensures that S_a will be gauge invariant, as we will see below. We initially account for a non-trivial coupling to the dilaton via the potential

$$Z(\lambda) = Z_0 \Big(1 + d \frac{\lambda^4}{\hat{\lambda}_0^4} \Big). \tag{4.24}$$

As we will see when studying the UV asymptotics of our model, this choice of potential does not produce the desired features of QCD and will need to be modified. This will be discussed in the next chapter.

In order to take into account the anomalous effects due to the external gauge fields in the boundary theory, V_μ, A_μ, we also need to include the Chern-Simons term [43] defined as

$$S_{\rm CS} = -\frac{M_p^3 N_c^2 x}{2}\int d^5x \tilde{\epsilon}^{MNPQR} A_M (3\kappa F^V_{NP}F^V_{QR} + \gamma F^A_{NP}F^A_{QR}) \tag{4.25}$$

where $\tilde{\epsilon}^{MNPQR}$ is the Levi-Civita symbol.

Gibbons-Hawking and Counterterm

We formally need to include two extra terms to the action. The first is the Gibbons-Hawking (GH), whose inclusion is necessary to make the variational problem of the metric well-defined on spacetimes with a boundary, such as AdS [37]. Its contribution reads

$$S_{\rm GH} = 2M_p^3 N_c^2 \int d^4x\sqrt{-h}K, \tag{4.26}$$

where

$$K_{\mu\nu} = \boldsymbol{\nabla}_\mu n_\nu = \frac{1}{2} n^\rho \partial_\rho h_{\mu\nu} \quad , \quad K = h^{\mu\nu} n_{\mu\nu}. \tag{4.27}$$

with $h_{\mu\nu}$ the induced metric on the bounary, n_μ the outward directed unit normal to the boundary and K is the extrinsic curvature. The second is the counterterm $S_{\rm CT}$, which we will not consider explicitly here [50]. Its presence is required to make the value for the on-shell action action on geometries with infinite volume such as the asymptotically AdS that we are considering finite.

4.3 Holographic Model

Putting everything together, the holographic action to be studied is stated in full as

$$S = S_g + S_f + S_a + S_{\rm CS} + S_{\rm GH} + S_{\rm CT}. \tag{4.28}$$

As the full equations of motion are quite cumbersome and provide no physical insight before an ansatz, presented in the next section is assumed, they are listed in the Appendix B. We make use of the holograhic prescription (4.12) to derive

the one point function[4]

$$\mathcal{J}_V^\mu = \lim_{r\to 0} \frac{M_p^3 N_c^2 x V_f(\lambda) w(\lambda)}{8} \sum_{k=+,-} \sqrt{-\det \boldsymbol{A}_k}\Big(\boldsymbol{A}_k^{-1\mu r} - \boldsymbol{A}_k^{-1 r\mu}\Big) + 6M_p^3 N_c^2 x\kappa \tilde{\epsilon}^{\sigma\nu\rho\mu r} A_\sigma \partial_\nu V_\rho, \tag{4.29}$$

which we identify as the consistent current defined in (3.33). Observing the response of this current to a perturbation will enable us to calculate the anomalous coefficients in Chapter 6.

Since the on-shell gravity action supplies us with information about the effective action of the boundary theory (3.20), we can find expressions for the anomaly coefficients in terms of the Chern-Simons coefficients, κ and γ. By anomaly coefficients a_i, we mean the numerical prefactors in the anomaly functions $\mathcal{A}_i$ whose definition should be clear from (3.15), (3.29) and (3.30). We will now observe how the holographic action transforms under the gauge transformation

$$V_M \to V_M + \partial_M \alpha, \tag{4.30}$$
$$A_M \to A_M + \partial_M \beta, \tag{4.31}$$
$$\mathfrak{a} \to \mathfrak{a} + x\beta. \tag{4.32}$$

Performing such a gauge transformation and using Stokes' theorem, we are left with the boundary term

$$-\frac{M_p^3 N_c^2 x}{2} \int d^4x \beta \epsilon^{\mu\nu\rho\sigma} (3\kappa F^V_{\mu\nu} F^V_{\rho\sigma} + \gamma F^A_{\mu\nu} F^A_{\rho\sigma}). \tag{4.33}$$

If we then perform both the chiral transformation and the gauge transformations

$$V_\mu \to V_\mu + \partial_\mu \alpha, \tag{4.34}$$
$$A_\mu \to A_\mu + \partial_\mu \beta \tag{4.35}$$

on the effective action of the QFT theory (3.20), we find that we are left with the term

$$-\int d^4x \epsilon^{\mu\nu\rho\sigma} \Big(\Big[\beta a_1 - \frac{N_f}{16\pi^2}\delta\theta\Big] \operatorname{tr}\big(G_{\mu\nu} G_{\rho\sigma}\big) + \beta a_2 F^V_{\mu\nu} F^V_{\rho\sigma} + \beta a_3 F^A_{\mu\nu} F^A_{\rho\sigma} \Big). \tag{4.36}$$

Firstly, note that we can actually cancel out the contribution from the gauge anomaly $\mathcal{A}_1$ by insisting that

$$\theta \to \theta + \frac{N_f}{16\pi^2}\delta\theta = \theta + \frac{N_f}{16\pi^2}\beta \tag{4.37}$$

[4]We do not consider the one point function $\mathcal{J}_A$ here as its computation requires us to solve the equations of motion in full. Moreover, we only need to know $\mathcal{J}_V$ in order to compute the CME, CSE and CVE.

We can then compare the two expressions (4.33), (4.36) to find that

$$\kappa = \frac{2a_2}{3M_p^3 N_c^2 x} \quad , \quad \gamma = \frac{2a_3}{M_p^3 N_c^2 x}. \tag{4.38}$$

The goal of this thesis is to compute anomalous conductivities, which should be given in terms of κ, γ. Using the above identifications, we can then compute the conductivites in terms of the anomaly coefficients. Consequently, the conductivities will take a form similar to (2.20).

Chapter 5

Holographic Background

As was discussed in Chapter 2, we will compute anomalous conductivities associated with the QGP by making use of linear response theory. In order to apply linear response, we will schematically write our holographic fields in the form background + fluctuation[1]

$$g = g_{\rm bg} + \delta g, \tag{5.1}$$

$$V = V_{\rm bg} + \delta \mathcal{V}, \tag{5.2}$$

$$A = A_{\rm bg} + \delta \mathcal{A}. \tag{5.3}$$

This chapter will contain an explicit, thorough explanation of how the background terms are chosen before evaluating the equations of motion, listed in Appendix B given such ansatz[2]. Following is an explanation detailing the construction of the numerical setup, specifically with relation to the choice of coordinates. We will study the UV asymptotics of the gauge fields and provide a comment related to the issue of our initial definition of $Z(\lambda)$. Lastly, we will briefly discuss some plots, which characterize the thermodynamics of the background.

5.1 Background Ansatz

We firstly state the reasoning behind our constuction of the background metric. As was mentioned before, we do not want to the bulk theory we consider to possess all of the symmetries of AdS. Therefore we need to adjust our ansatz for the metric so that it is asymptotically AdS, while at the same time breaking some of these symmetries as we go further into the IR. The general ansatz we presume is

$$ds^2 = e^{2a(r)}\Big(- f(r)dt^2 + \frac{1}{f(r)}dr^2 + dx_i dx^i \Big). \tag{5.4}$$

[1] We do not consider fluctuations of the axion or dilaton.

[2] Linear response on this background will then be performed in the next chapter.

The asymptotic UV behaviour of the warp factor $e^{2a(r)}, a \in [0, \infty)$ and the blackening factor $f(r)$ are fixed by demanding that

$$\lim_{r\to 0} e^{2a(r)} = \frac{L^2}{r^2} \quad , \quad \lim_{r\to 0} f(r) = 1 \tag{5.5}$$

so as to match with (4.3).

The choice of background directly affects the nature of the potential influencing two test quarks. As we are trying to describe the plasma phase of QCD, we want the force between quarks to disappear at large distances. This is done by considering a black hole solution [51] characterized by the existence of a non-extremal horizon at r_h and the vanishing of the blackening factor at said horizon. Furthermore, the Hawking temperature of this black hole [37] is

$$\frac{T}{\Lambda} = -\frac{f'(r_h)}{4\pi}, \tag{5.6}$$

which is naturally identified with the temperature of the QGP we are considering[3]. The constant Λ is related to Λ_{QCD}, which is set to 1 in the numerical solver. Nevertheless, we include it in our definition for the sake of clarity and because we eventually want to plot dimensionless quantities.

It has been proposed [37] that finite density and chemical potential are introduced by allowing for a non-trivial profile for the time component of the gauge field in the radial direction

$$V_{\mathrm{bg}} = V_t(r)dt \quad , \quad A_{\mathrm{bg}} = A_t(r)dt. \tag{5.7}$$

In its most elementary definition the chemical potential is the energy needed to add one unit of charge to the thermal ensemble. Since the thermal ensemble is represented by a black hole, one can define the addition of a unit of charge by transporting such a charge from infinity to behind the horizon. It then seems natural to identify the vector chemical potentials as[4]

$$\mu_V = V_t(r_h) - V_t(0) \tag{5.8}$$

However there exists further gauge freedom, which allows us to set the temporal components of the gauge fields to zero at the horizon, leaving us with chemical potential

$$\mu_V = -V_t(0) \tag{5.9}$$

With the above definitions in mind, we can go on and evaluate the equations of motion, which are presented below.

[3] The appearance of a minus sign in the definition of temperature is an artifact of the coordinate system where $r \to 0$ in the UV.

[4] The situation for the axial chemical potential is more complicated and will be treated in detail later in the chapter.

5.2 Background Equations of Motion

Maxwell and Axion Equations

All components of the background vector and axial gauge equations are zero apart from the time components, which immediately implies that $\partial_r \mathfrak{a} = \partial_i \mathfrak{a} = 0$. We will discuss the time dependence of the axion below. For the moment, the vector and axial equations are listed respectively as

$$0 = \partial_r \Big[\frac{x V_f(\lambda) w^2(\lambda)}{4} \sum_{k=+,-} \sqrt{-\det \boldsymbol{A}_k} \frac{V_t' \pm A_t'}{e^{4a(r)} - w^2(\lambda)(V_t' \pm A_t')^2} \Big] \tag{5.10}$$

and

$$\begin{aligned} 0 = \partial_r \Big[\frac{x V_f(\lambda) w^2(\lambda)}{4} \sum_{k=+,-} k \sqrt{-\det \boldsymbol{A}_k} \frac{V_t' \pm A_t'}{e^{4a(r)} - w^2(\lambda)(V_t' \pm A_t')^2} \Big] \\ + \frac{Z(\lambda) e^{3a(r)}}{f(r)} (\partial_t \mathfrak{a} - 2x A_t) \end{aligned} \tag{5.11}$$

where X' denotes a derivative with respect to r. To clear up any possible confusion, the appearance of $\pm$ indicates that a $+$ appears in the $k = +$ term and that a $-$ appears in the $k = -$ term. The determinant factor's explicit appearance through such a background ansatz is

$$\sqrt{-\det \boldsymbol{A}_k} = e^{10a(r)} - e^{6a(r)} w^2(\lambda)(V_t' \pm A_t')^2. \tag{5.12}$$

For future reference, it will be convenient to define

$$Q^+ = \frac{x V_f(\lambda) w^2(\lambda)}{2} \sqrt{-\det \boldsymbol{A}_+} \frac{V_t' + A_t'}{e^{4a(r)} - w^2(\lambda)(V_t' + A_t')^2}, \tag{5.13}$$

$$Q^- = \frac{x V_f(\lambda) w^2(\lambda)}{2} \sqrt{-\det \boldsymbol{A}_-} \frac{V_t' - A_t'}{e^{4a(r)} - w^2(\lambda)(V_t' - A_t')^2} \tag{5.14}$$

so that the Maxwell equations can be written as

$$0 = \partial_r \Big[\frac{1}{2}(Q^+ + Q^-) \Big], \tag{5.15}$$

$$0 = \partial_r \Big[\frac{1}{2}(Q^+ - Q^-) \Big] + \frac{Z(\lambda) e^{3a(r)}}{f(r)} (\partial_t \mathfrak{a} - 2x A_t). \tag{5.16}$$

We can use the above information to fully determine the behaviour of the axion. In particular, with the knowledge that the axion only possesses time dependence we conclude that

$$\partial_t^2 \mathfrak{a} = 0, \tag{5.17}$$

which admits the solution

$$\mathfrak{a}(t) = \mathfrak{a}_0 + x \mathfrak{a}_1 t, \tag{5.18}$$

where $\mathfrak{a}_0, \mathfrak{a}_1$ are constants. In fact, because the axion only appears through a constant contribution to the action (4.23), we will neglect it from this point onwards.

Einstein Equations

There are three independent components of the background Ricci tensor: R_{tt}, R_{rr} and R_{xx}. They read

$$\begin{aligned} R_{tt} &= 3f(r)(a'(r))^2 + \frac{5}{2}f'(r)a'(r) + f(r)a''(r) + \frac{1}{2}f''(r) \\ &= \frac{1}{3}V_g(\lambda)e^{2a(r)} + 2\frac{Z(\lambda)}{f(r)}(xA_t)^2 \\ &- \frac{xV_f(\lambda)e^{-3a(r)}}{12}\sum_{k=+,-}\sqrt{-\det \boldsymbol{A}_k}\frac{2e^{4a(r)} - 3w^2(\lambda)(V_t' \pm A_t')^2}{e^{4a(r)} - w^2(\lambda)(V_t' \pm A_t')^2}, \end{aligned} \tag{5.19}$$

$$\begin{aligned} R_{rr} &= -\frac{5}{2}f'(r)a'(r) - 4f(r)a''(r) - \frac{1}{2}f''(r) \\ &= -\frac{1}{3}V_g(\lambda)e^{2a(r)} + \frac{4\lambda'^2}{3\lambda^2}f(r) \\ &+ \frac{xV_f(\lambda)e^{-3a(r)}}{12}\sum_{k=+,-}\sqrt{-\det \boldsymbol{A}_k}\frac{2e^{4a(r)} - 3w^2(\lambda)(V_t' \pm A_t')^2}{e^{4a(r)} - w^2(\lambda)(V_t' \pm A_t')^2}, \end{aligned} \tag{5.20}$$

$$\begin{aligned} R_{xx} &= 3f(r)(a'(r))^2 + f'(r)a'(r) + f(r)a''(r) \\ &= \frac{1}{3}V_g(\lambda)e^{2a(r)} \\ &- \frac{xV_f(\lambda)e^{-3a(r)}}{6}\sum_{k=+,-}\sqrt{-\det \boldsymbol{A}_k}\frac{e^{4a(r)}}{e^{4a(r)} - w^2(\lambda)(V_t' \pm A_t')^2}. \end{aligned} \tag{5.21}$$

From the equations above along with (5.10) and (5.11) we can derive the useful relations

$$0 = \frac{2Z(\lambda)(xA_t)^2}{f^2(r)} + 3a''(r) - 3(a'(r))^2 + \frac{4\lambda'^2}{3\lambda^2} \tag{5.22}$$

$$0 = \partial_r\Big[f'(r)e^{3a(r)} - V_t(Q^+ + Q^-) - A_t(Q^+ - Q^-)\Big]. \tag{5.23}$$

Finally, one can add the Einstein equations and then differentiate with respect to λ to get the equation of motion for the dilaton. It can also be computed by varying the holographic action with respect to λ and then evaluating it on the holographic background. We include the dilaton equation for completeness

$$\begin{aligned} 0 &= \frac{8}{3\lambda}\partial_r\Big[e^{3a(r)}f(r)\lambda'\Big] + e^{5a(r)}\frac{dV_g(\lambda)}{d\lambda} + \frac{2}{f(r)}e^{3a(r)}\frac{dZ(\lambda)}{d\lambda}(xA_t)^2 \\ &- \frac{1}{2}x\frac{dV_f(\lambda)}{d\lambda}\sum_{k=+,-}\sqrt{-\det \boldsymbol{A}_k} \\ &+ \frac{1}{2}xV_f(\lambda)w(\lambda)\frac{dw(\lambda)}{d\lambda}\sum_{k=+,-}\sqrt{-\det \boldsymbol{A}_k}\frac{(V_t' \pm A_t')^2}{e^{4a(r)} - w^2(\lambda)(V_t' \pm A_t')^2}, \end{aligned} \tag{5.24}$$

although it will not be relevant in what follows.

5.3 Construction of Numerical Solution

We will solve both the background and fluctuation equations numerically. Anticipating the numerical issues that will arise due to taking the limit $r \to 0$ in the UV, we make a suitable change of coordinates [41], writing all of our fields in term of the exponent of the warp factor, a. The change of coordinates is defined through the relation

$$q = e^a \frac{dr}{da}. \tag{5.25}$$

To clean up the equations of motion, it makes sense to define[5]

$$\sqrt{-\det \tilde{\boldsymbol{A}}_k} = e^{2a} - \big(\frac{w(\lambda)}{q}\big)^2 (\dot{V}_t \pm \dot{A}_t)^2, \tag{5.26}$$

where $\dot{X}$ denotes a derivative with respect to a. In a coordinates Q^+ and Q^- are then

$$Q^+ = \frac{x V_f(\lambda) w^2(\lambda) e^{3a} (\dot{V}_t + \dot{A}_t)}{2q\sqrt{-\det \tilde{\boldsymbol{A}}_+}}, \tag{5.27}$$

$$Q^- = \frac{x V_f(\lambda) w^2(\lambda) e^{3a} (\dot{V}_t - \dot{A}_t)}{2q\sqrt{-\det \tilde{\boldsymbol{A}}_-}}. \tag{5.28}$$

We now go on and respectively rewrite the Maxwell equations (5.15), (5.16) along with three equations from the gravity sector: (5.21), eq5.22 and (5.22) in these coordinates[6]

$$0 = \partial_a \Big[\frac{1}{2}(Q^+ + Q^-)\Big], \tag{5.29}$$

$$0 = \partial_a \Big[\frac{1}{2}(Q^+ - Q^-)\Big] - 2xq \frac{Z(\lambda) e^{2a}}{f(a)} A_t, \tag{5.30}$$

$$\dot{f}(a) + f(a)\Big(4 - \frac{\dot{q}}{q}\Big) = \frac{1}{3} V_g(\lambda) q^2 - \sum_{k=+,-} \frac{x V_f(\lambda) e^a q^2}{6\sqrt{-\det \tilde{\boldsymbol{A}}_k}}, \tag{5.31}$$

$$0 = \frac{2Z(\lambda)(xA_t)^2}{f^2(a)} + 3e^{2a}\Big(1 + \frac{\dot{q}}{q}\Big) - 3\frac{e^{2a}}{q^2} + \frac{4e^{2a}\dot{\lambda}^2}{3q^2\lambda^2}, \tag{5.32}$$

$$0 = \partial_a \Big[\frac{e^{4a}}{q}\dot{f}(a) - V_t(Q^+ + Q^-) - A_t(Q^+ - Q^-)\Big]. \tag{5.33}$$

These will be the five equations that we will use to solve for $V_t(a)$, $\dot{V}_t(a)$, $A_t(a)$, $\dot{A}_t(a)$, $f(a)$, $\dot{f}(a)$, $q(a)$ and $\lambda(a)$. We will integrate from $a = 0$ to $a = a_{\text{cut}}$, where a_{cut} is interpreted as a UV cutoff. Therefore, we need to specify the boundary conditions $\dot{V}_{th}$, $\dot{A}_{th}$, $\dot{f}_h$, q_h and λ_h in addition to the assumptions

[5] In what follows, the matrix $\tilde{\boldsymbol{A}}$ itself is of no concern to us. The definition of its determinant just allows us to simplify the equations of motion slightly.

[6] As was mentioned previously, we will not include the axion term.

$V_{th} = A_{th} = f_h = 0$[7], which were justified in the previous section.

We enforce the conventional boundary condition by setting $\dot{f}(0) = 1$. Expanding (5.31) at the horizon and demanding regularity yields the condition

$$q_h^2 = \frac{6}{2V_g(\lambda_h) - xV_f(\lambda_h)\sum_{k=+,-}\frac{1}{\sqrt{1-(w(\lambda_h q_h^{-1}))^2(\dot{V}_{th}\pm\dot{A}_{th})^2)}}}. \tag{5.34}$$

From (5.25), we can see that we should take the negative branch as the definition of q_h. There is obviously the issue that q_h is written in terms of itself. This is rectified by defining the horizon values of the derivatives of the gauge fields as

$$Q^V = q_h^{-1}\dot{V}_{th} \quad , \quad Q^A = q_h^{-1}\dot{A}_{th}. \tag{5.35}$$

An initial choice of Q^V, Q^A then automatically determines q_h, $\dot{V}_{th}$ and $\dot{A}_{th}$. The value of λ_h is then regarded as a free parameter, whose behaviour we will study in the final section of this chapter.

Scaling Symmetries

It is necessary to produce the UV behaviour (5.5) in order to construct an asymptotically AdS spacetime. This is done by first noticing that the equations of motion are invariant under

- The scaling of f. The following quantities scale as:
  $f \to \frac{f}{\delta_f^2}$,$q \to \frac{q}{\delta_f}$, $V_t \to \frac{V_t}{\delta_f}$, $A_t \to \frac{A_t}{\delta_f}$

- The scaling of a. The following quantities scale as:
  $a \to a + \delta_a$, $V_t \to V_t e^{\delta_a}$, $A_t \to A_t e^{\delta_a}$

The number δ_f is computed by reading the unscaled $\tilde{f}(a_{\text{cut}})$ from the output of the numerical solution, before solving

$$\delta_f^2 = \frac{\tilde{f}(a_{\text{cut}})}{f(a_{\text{cut}})}, \tag{5.36}$$

where we have demanded that $f(a_{\text{cut}}) = 1$.

From [52], the UV expansion of the unscaled a_{us} is

$$a^{\text{us}} = a_0 + \frac{1}{b_0\lambda} + \frac{b_1}{b_0^2}\ln(b_0\lambda) + \mathcal{O}(\lambda) \tag{5.37}$$

[7] To avoid numerical issues we impose an IR cutoff, $\epsilon \sim 10^{-7}$ and set $V_{th} = A_{th} = f_h = \epsilon$.

where the b_i's are coefficients of the QCD beta function, a_0 is a constant of integration and the asymptotic expansion of the dilaton is

$$\lambda = -\frac{1}{b_0 \ln(r\Lambda)} + \mathcal{O}\Big(\frac{\ln\big(-\ln(r\Lambda)\big)}{\ln(r\Lambda)^2}\Big). \tag{5.38}$$

We will scale our solution in such a way that the integration constant is zero. Therefore, it is necessary to first define

$$\delta a = \log L - a_{\text{cut}} + \frac{1}{b_0\lambda} + \frac{b_1}{b_0^2}\ln(b_0\lambda) \tag{5.39}$$

and then scale appropriately with δa as described above to produce the desired asymptotics.

5.4 Gauge Field Asymptotics

Even though we are solving the system numerically in a coordinates, we will define the chemical potentials μ_v, μ_A in r coordinates as to agree with more general conventions. From the background equations (5.10), (5.11), it can be shown that the asymptotic behaviour of the gauge fields is

$$\lim_{r\to 0} V_t \sim -\mu_V + \tilde{V} r^2 \tag{5.40}$$

$$\lim_{r\to 0} A_t \sim -\mu_A r^{\Delta} \ln r^p + \tilde{A} r^{2-\Delta} \ln r^{-p} \tag{5.41}$$

With these definitions, we now go to a coordinates using (5.37) and (5.38). At leading order, we can then write

$$e^a = \frac{L}{r}. \tag{5.42}$$

In a coordinates, the asymptotic expansions of the vector gauge field is

$$\lim_{a\to\infty} V_t \sim -\mu_V + \tilde{V} L^2 e^{-2a} \tag{5.43}$$

The vector chemical potential can then be read easily from the constant behaviour of V_t.

The situation for the axial gauge field is more complicated. For such a massive field, the asymptotic behaviour in a coordinates is

$$\lim_{a\to\infty} A_t \sim -\mu_A e^{-\Delta a} L^{\Delta} a^{-p} + \tilde{A} e^{(\Delta-2)a} a^p. \tag{5.44}$$

If we then expand (5.30) near the UV, we can use the expansions (5.38) and

$$q = -L\Big(1 - \frac{4}{9a} + \mathcal{O}\Big(\frac{1}{a^2}\Big)\Big) \tag{5.45}$$

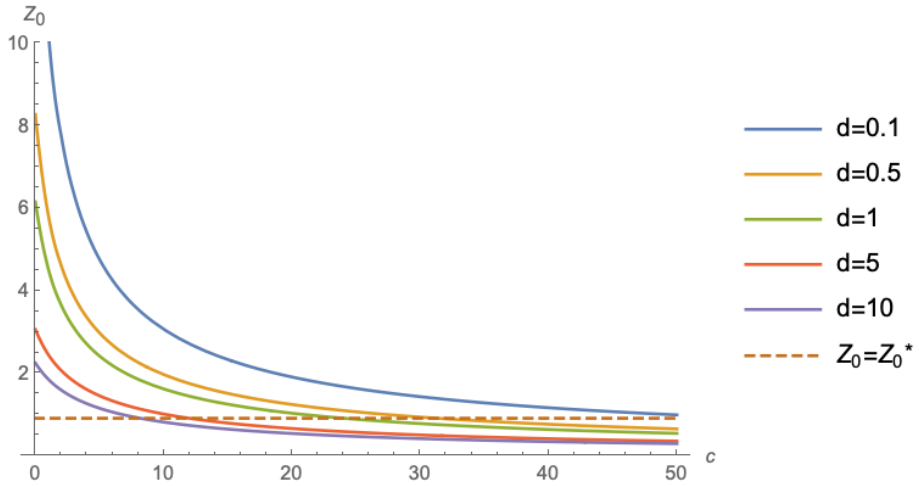

Figure 5.1: Behaviour of Z_0 as a function of c for different values of d. It turns out that we need to increase c, d to at least $\mathcal{O}(1)$ to push Z_0 below Z_0^*.

from [41] to calculate Δ, p. Expanding up to zeroth order, our result is

$$\Delta = 1 - \sqrt{1 + \frac{4Z_0 x L^2}{W_0 w^2(\lambda_0)}} \tag{5.46}$$

where λ_0 is the value of the dilaton at the UV boundary. To completely determine Δ, we should compute Z_0 independently using our numerically generated background. This coefficient Z_0 can be fixed by computing the topological susceptibility in pure Yang-Mills [53] and such details are put in Appendix A. Recalling the definition of $Z(\lambda)$, (4.24) with $d = 0.1$, $L = 1/\sqrt{1 - 5/24}$ we calculate $Z_0 \sim 16.4$, implying $\Delta \sim -6.434$.

Let us pause and consider the physical meaning of Δ in our boundary theory [49]. The normalizable mode of (5.44) is identified with the associated current of the QFT, $\mathcal{J}_A^\mu$ via the holographic prescription. The conformal dimension of this current is

$$\dim(\tilde{A}) = [\mathcal{J}_A^\mu] = 3 - \Delta \tag{5.47}$$

where $\Delta \leq 0$. This implies that we need to demand $\Delta \leq -1$. Otherwise the dual operator will be irrelevant in the IR and the AdS asymptotics will be destroyed. For this reason, we henceforth refer to Δ as the anomalous dimension. Furthermore, our previous calculation of $\Delta \sim -6.434$ clearly does not satisfy this requirement. In fact, we can solve (5.46) with $\Delta = -1$ to show that $Z_0 \leq 0.906 = Z_0^*$, the critical value of Z_0. It will not be possible to go below this critical value with a "natural" choice[8] of the coefficient, d.

[8] By natural, we mean a value, which can be justified through comparison with experimental or lattice data.

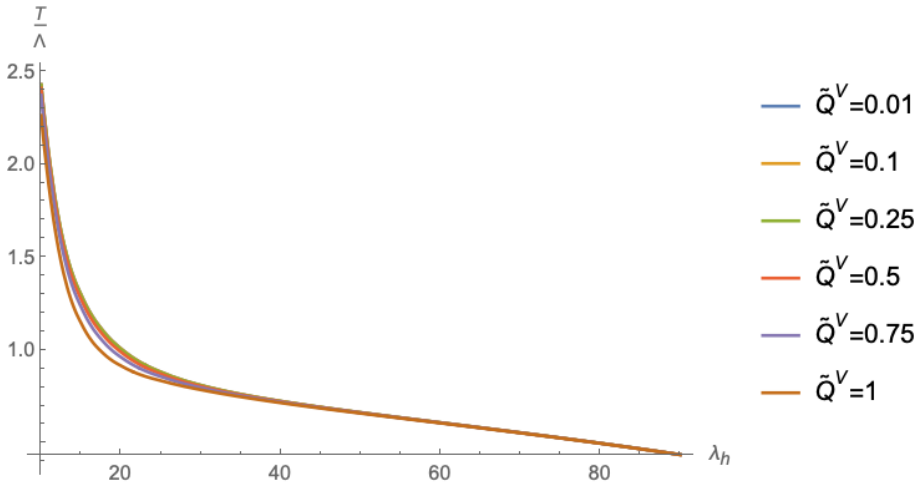

Figure 5.2: Behaviour of T as a function of λ_h for small, fixed $\tilde{Q}^A$. The curves converge to the $\tilde{Q}^V = 0$ curve as $\tilde{Q}^V$ is decreased.

We attempt to fix this problem by adding a linear term to the potential $Z(\lambda)$. The potential is redefined as [53]

$$Z(\lambda) = Z_0\Big(1 + c\frac{\lambda}{\tilde{\lambda}_0} + d\frac{\lambda^4}{\tilde{\lambda}_0^4}\Big). \tag{5.48}$$

This seems to work quite well. As is summarized in Fig (5.1), it is possible to obtain a $Z_0 < Z_0^*$ by tweaking c and d appropriately. We intend on matching these coefficients to some physical quantities computed from lattice QCD in the future[9]. For the sake of this thesis however, we will just choose a setup, which does not destroy the AdS asymptotics. In addition, we need to ensure we avoid any numerical issues that could be produced by taking Δ too close to -1. Therefore, we choose $Z_0 = 0.57$ with $c = 18$ and $d = 10$. This determines $\Delta = -0.7$.

Expanding (5.30) up to $\mathcal{O}(1/a)$ analytically determines the value of p as

$$p = -2\frac{b_0\tilde{\lambda}_0\Big(4L^2Z_0 + 3w_0^2\Delta(\Delta-2)(W_0+W_1\lambda)\Big) - 9cL^2Z_0}{9b_0\tilde{\lambda}_0 w_0^2(\Delta-1)(W_0+W_1\lambda)}. \tag{5.49}$$

Plugging in all of the V-QCD coefficients along with coefficients from our numerical solution, we calculate $p = -1.82$, The coefficients W_1, w_0, $\tilde{\lambda}_0$ are defined in Appendix A and the choices of Z_0, Δ, c, L have been mentioned above. The value of $b_0 = 3/8\pi^2$ is taken from [52]. Given the numerical values of Δ, p we can calculate the value of μ_A by plotting $A_t e^{\Delta a} L^{-\Delta} a^p$ and reading its constant value at large a.

[9] We will elaborate as to what exactly is meant by this in the Conclusion 7.

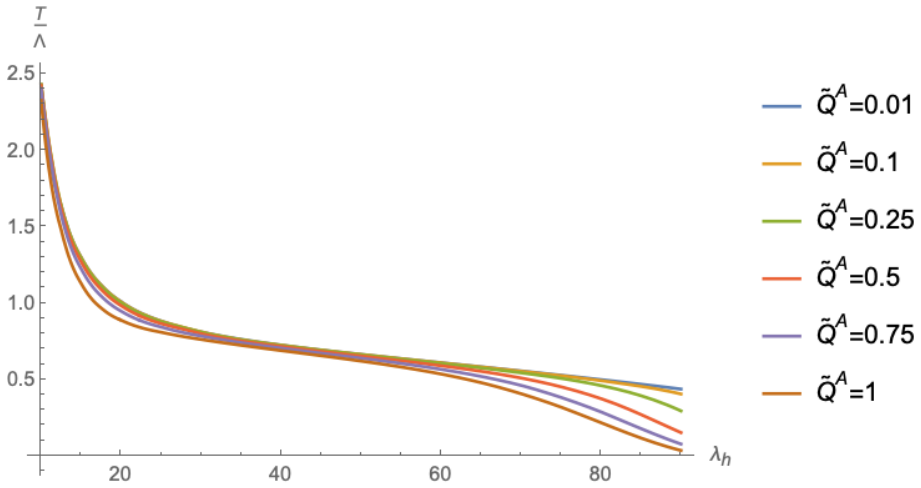

Figure 5.3: Behaviour of T as a function of λ_h for small, fixed $\tilde{Q}^V$. The curves converge to the $\tilde{Q}^A = 0$ curve as $\tilde{Q}^A$ is decreased. Note that the curves fall off at lower λ_h when the unscaled axial charge is larger.

5.5 Background Analysis

This chapter is concluded by a few comments related to the plots 5.2, 5.3, 5.4 and 5.5. It should be noted that because the chemical potentials are the outputs of our numerical solver, they are more difficult to fix. This is why we instead choose to fix the unscaled charges $\tilde{Q}^V, \tilde{Q}^A$. For the sake of brevity, we write these in terms of the scaled charges

$$\tilde{Q}^V = Q^V \frac{\Lambda}{s^{\frac{1}{3}}} \tag{5.50}$$

$$\tilde{Q}^A = Q^A \frac{\Lambda}{s^{\frac{1}{3}}} \tag{5.51}$$

where s, the entropy density is defined as [37]

$$\frac{s}{\Lambda^3} = \exp(3\delta a) \tag{5.52}$$

There is not much to be learned from the plots 5.2, 5.4 other than the fact that the choice of vector charge does not have a significant impact on the background's thermodynamics, at least in comparison to the choice of axial charge. In particular, one can see that the family curves in Fig 5.2 converge to the $\tilde{Q}^V = 0$ curve at a much faster rate than in Fig 5.3, where they converge to the $\tilde{Q}^A = 0$ curve. The significantly larger backreaction of the field A_M on the gravitational background can be traced back to the fact that it is massive.

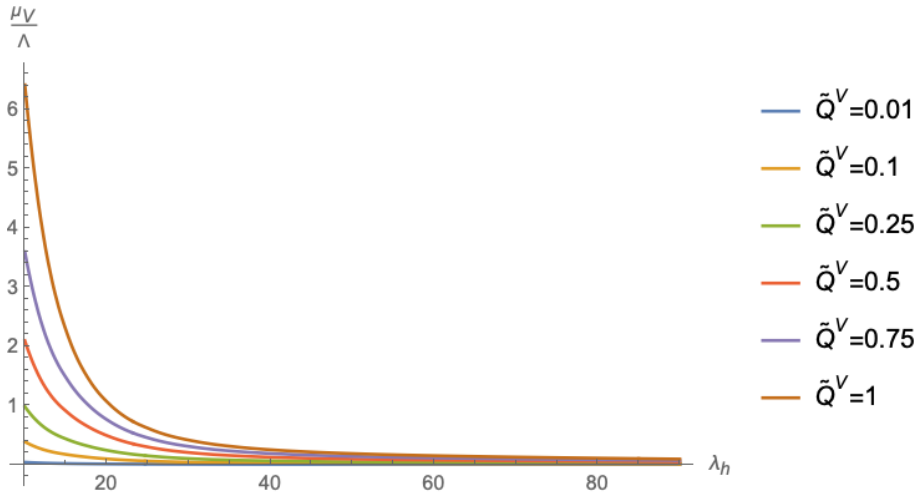

Figure 5.4: Behaviour of μ_V as a function of λ_h for small, fixed $\tilde{Q}^A$. Clearly, the value of unscaled vector charge only impacts the vector chemical potential at high temperatures. Note that the curves fall off at lower λ_h when the unscaled axial charge is larger.

The complete decay of temperature in the plots 5.2, 5.3 is cut out at $\lambda_h = 90$. The reason for this is that at such a low temperature, the QGP phase should not be the dominating phase. There is potential to study this behaviour further by the inclusion of the tachyon. This will be elaborated on further in the Conclusion 7.

It is easy to see that in Fig 5.5, the curves level out for smaller λ_h, the larger the value of $\tilde{Q}^A$. This is in contrast to the case in Fig 5.3 where the temperature curves decay at lower λ_h the larger the value of $\tilde{Q}^A$. As was mentioned already, this demonstrates the fact that the value of $\tilde{Q}^A$ significantly impacts the background thermodynamics. It is also possible to infer from nonmonotonic nature of the curves in Fig 5.5 that there may be some kind of phase coexistence. However, without further analysis of the system's thermodynamics, not much more can be said about this.

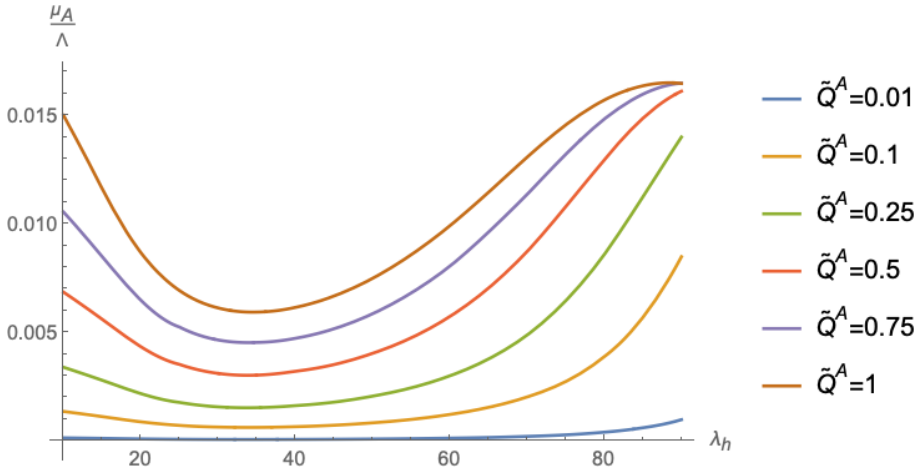

Figure 5.5: Behaviour of μ_A as a function of λ_h for small, fixed $\tilde{Q}^V$. The behaviour of the axial chemical potential could be indicative of some non trivial phase behaviour.

Chapter 6

Anomalous Conductivities

In this final chapter we will present the main results of the thesis. We will observe the response of suitably defined fluctuations on the background explored in the previous chapter. This will allow us to compute the anomalous conductivities associated with the CME, CSE and CVE.

We consider the following ansatz for the fluctuations

$$\delta g_{tx} = e^{2a(r)}(\delta h_1(r)z + \delta h_2(r)) \quad , \quad \delta g_{ty} = e^{2a(r)}(\delta l_1(r)z + \delta l_2(r)) \tag{6.1}$$

$$\delta \mathcal{V}_x = \delta V_{x1}(r)z + \delta V_{x2}(r) \quad , \quad \delta \mathcal{V}_y = \delta V_{y1}(r)z + \delta V_{y2}(r) \tag{6.2}$$

$$\delta \mathcal{A}_x = \delta A_{x1}(r)z + \delta A_{x2}(r) \quad , \quad \delta \mathcal{A}_y = \delta A_{y1}(r)z + \delta A_{y2}(r) \tag{6.3}$$

where the perturbations are assumed to be wave-like with their momentum oriented in the z direction. We have assumed constant magnetic field and vorticity so that the fluctuations have no time dependence and only depend linearly on z. The fact that we are only considering linear response implies that none of the fluctuations will couple to other fluctuations. Therefore, as we are only interested in studying the impact of the dilaton on the background, its fluctuation can be turned off in a consistent way.

6.1 Fluctuation Equations of Motion

We now list the equations of motion for the fluctuations defined above. As we intend to solve the fluctuation equations numerically, it is convenient to immediately present the equations in a coordinates.

Maxwell Equations

For all of the fluctuating fields, only the x, y components of the equations are non-zero. We start by listing the equation of motion for the vector fluctuations.

The x and y components are

$$-6\kappa(\partial_z\delta\mathcal{V}_y\dot{A}_t+\dot{V}_t\partial_z\delta\mathcal{A}_y)=\partial_a\Big[\frac{xV_f(\lambda)w^2(\lambda)e^{3a}}{4q}\sum_{k=+,-}\frac{f(r)(\delta\dot{\mathcal{V}}_x\pm\delta\dot{\mathcal{A}}_x)}{\sqrt{-\det\boldsymbol{A}_k}}\Big]+\frac{1}{2}\delta\dot{g}_{tx}(Q^++Q^-) \tag{6.4}$$

and

$$6\kappa(\partial_z\delta\mathcal{V}_x\dot{A}_t+\dot{V}_t\partial_z\delta\mathcal{A}_x)=\partial_a\Big[\frac{xV_f(\lambda)w^2(\lambda)e^{3a}}{4q}\sum_{k=+,-}\frac{f(r)(\delta\dot{\mathcal{V}}_y\pm\delta\dot{\mathcal{A}}_y)}{\sqrt{-\det\boldsymbol{A}_k}}\Big]+\frac{1}{2}\delta\dot{g}_{ty}(Q^++Q^-) \tag{6.5}$$

respectively, where we have used the definitions of $Q^\pm$ and (5.29). Similarly, for the axial gauge field they are

$$2Z(\lambda)x^2qe^{2a}\delta\mathcal{A}_x+2\Big(3\kappa\partial_z\delta\mathcal{V}_y\dot{V}_t+2\gamma\partial_z\delta\mathcal{A}_y\dot{A}_t\Big)=\partial_a\Big[\frac{xV_f(\lambda)w^2(\lambda)e^{3a}}{4q}\sum_{k=+,-}k\frac{f(r)(\delta\dot{\mathcal{V}}_x\pm\delta\dot{\mathcal{A}}_x)}{\sqrt{-\det\boldsymbol{A}_k}}\Big]+\frac{1}{2}\delta\dot{g}_{tx}(Q^+-Q^-) \tag{6.6}$$

and

$$2Z(\lambda)x^2qe^{2a}\delta\mathcal{A}_y-2\Big(3\kappa\partial_z\delta\mathcal{V}_x\dot{V}_t+2\gamma\partial_z\delta\mathcal{A}_x\dot{A}_t\Big)=\partial_a\Big[\frac{xV_f(\lambda)w^2(\lambda)e^{3a}}{4q}\sum_{k=+,-}k\frac{f(r)(\delta\dot{\mathcal{V}}_y\pm\delta\dot{\mathcal{A}}_y)}{\sqrt{-\det\boldsymbol{A}_k}}\Big]+\frac{1}{2}\delta\dot{g}_{ty}(Q^+-Q^-). \tag{6.7}$$

Einstein Equations

Using the background equations, the Einstein equations simplify to

$$\delta\dot{\mathcal{V}}_x(Q^++Q^-)+\delta\dot{\mathcal{A}}_x(Q^+-Q^-)+\delta\mathcal{A}_x\partial_a(Q^+-Q^-)=\frac{e^{4a}}{q}\Big(\frac{\delta\dot{g}_{tx}\dot{q}}{q}-\delta\ddot{g}_{tx}-4\delta\dot{g}_{tx}\Big), \tag{6.8}$$

$$\delta\dot{\mathcal{V}}_y(Q^++Q^-)+\delta\dot{\mathcal{A}}_y(Q^+-Q^-)+\delta\mathcal{A}_y\partial_a(Q^+-Q^-)=\frac{e^{4a}}{q}\Big(\frac{\delta\dot{g}_{ty}\dot{q}}{q}-\delta\ddot{g}_{ty}-4\delta\dot{g}_{ty}\Big), \tag{6.9}$$

which can both be integrated to yield

$$\partial_a\Big[\delta\mathcal{V}_x(Q^+ + Q^-) + \delta\mathcal{A}_x(Q^+ - Q^-)\Big] = \partial_a\Big[-\frac{e^{4a}\delta\dot{g_{tx}}}{q}\Big], \tag{6.10}$$

$$\partial_a\Big[\delta\mathcal{V}_y(Q^+ + Q^-) + \delta\mathcal{A}_y(Q^+ - Q^-)\Big] = \partial_a\Big[-\frac{e^{4a}\delta\dot{g_{ty}}}{q}\Big]. \tag{6.11}$$

Consistent Current Response

We derive the form of the fluctuation of the relevant one-point function, from which we will read off the conductivities. The equation of motion for the field $\delta\mathcal{V}$ can be schematically rewritten as

$$\delta\mathcal{J}^\mu_V = \delta\tilde{\mathcal{J}}^\mu_V - \delta\Big(\partial_\nu\frac{\delta S}{\delta F^V_{\nu\mu}}\Big) \tag{6.12}$$

where $\delta\mathcal{J}^\mu_V$ is the fluctuation of the current defined in (4.29) and $\delta\tilde{\mathcal{J}}^\mu_V$ is the same expression evaluated at the horizon (as opposed to the boundary). Assuming our fluctuation ansatz, the only non-zero components of $\delta\tilde{\mathcal{J}}^\mu_V$ are just (6.4) and (6.5). We note that $f(a)$ vanishes at the horizon by definition. We also require δg_{tx} to vanish at the horizon to ensure the regularity of our solution[1] [21]. Therefore, $\delta\tilde{\mathcal{J}}^\mu_V = 0$ and we are left with

$$\delta\mathcal{J}^x_V = 4a_2\int_0^{a_{\text{cut}}} da(A_t\partial_z\delta\dot{\mathcal{V}}_y - \dot{V}_t\partial_z\delta\mathcal{A}_y), \tag{6.13}$$

$$\delta\mathcal{J}^y_V = -4a_2\int_0^{a_{\text{cut}}} da(A_t\partial_z\delta\dot{\mathcal{V}}_x - \dot{V}_t\partial_z\delta\mathcal{A}_x), \tag{6.14}$$

where we have used (4.38) to express the fluctuations in terms of anomaly coefficients. The appearance of this one-point function implies that we do not need to solve the full set of equations above in order to read off the conductivities. Let us now explain why this is so. Firstly, note that the one-point function only depends on z derivatives of the fluctuations. Then, if we expand all of our equations of motion above in the form

$$F(a) + zG(a) = 0, \tag{6.15}$$

we can just use the coefficient of z and hence, write the equations of motion in terms of δh_1,δl_1, δV_{x1}, δV_{y1}, δA_{x1} and δA_{y1}.

This realization significantly simplifies our task of solving the equations of

[1] We can actually show this independently by writing (6.4), (6.5) in the form (6.15) and using that $f(a) = 0$ at the horizon.

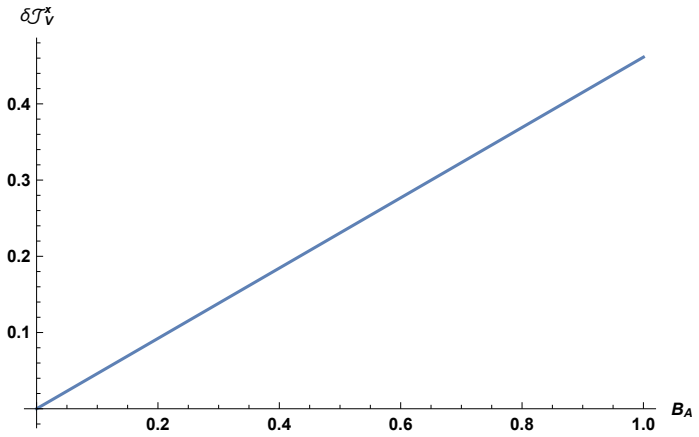

Figure 6.1: Exhibition of the linear dependence of the response current (6.13) on B_A. This implies that there will be a response associated with the source B_A, namely the CSE.

motion numerically. The input for the numerical solver is

$$0 = \partial_a\Big[\frac{xV_f(\lambda)w^2(\lambda)e^{3a}}{4q}\sum_{k=+,-}\frac{f(r)(\delta\dot{V}_{x1}\pm\delta\dot{A}_{x1})}{\sqrt{-\det\boldsymbol{A}_k}}\Big] + \frac{1}{2}\delta\dot{h}_1(Q^+ + Q^-), \tag{6.16}$$

$$2Z(\lambda)x^2qe^{2a}\delta A_{x1} = \partial_a\Big[\frac{xV_f(\lambda)w^2(\lambda)e^{3a}}{4q}\sum_{k=+,-}k\frac{f(r)(\delta\dot{V}_{x1}\pm\delta\dot{A}_{x1})}{\sqrt{-\det\boldsymbol{A}_k}}\Big] + \frac{1}{2}\delta\dot{h}_1(Q^+ - Q^-), \tag{6.17}$$

$$\partial_a\Big[\delta V_{x1}(Q^+ + Q^-)+\delta A_{x1}(Q^+ - Q^-)\Big] = \partial_a\Big[-\frac{e^{4a}\delta\dot{h}_1}{q}\Big]. \tag{6.18}$$

Note that because the Chern-Simons terms are no longer needed, the x and y components of the equations essentially coincide. The above three equations can be solved to compute δV_{x1}, δA_{x1}, $\delta\dot{V}_{x1}$ and $\delta\dot{A}_{x1}$, which is all that is needed in order to calculate the response to the consistent current (4.29). We also need to supply the boundary conditions[2] δV_{x1h}, δA_{x1h}, $\delta\dot{V}_{x1h}$ and $\delta\dot{A}_{x1h}$. Moreover, $\delta\dot{h}_{1h}$ will be a free parameter.

[2]Recall that we have demanded $\delta g_{txh} = 0$, which imples that $\delta h_{1h} = 0$.

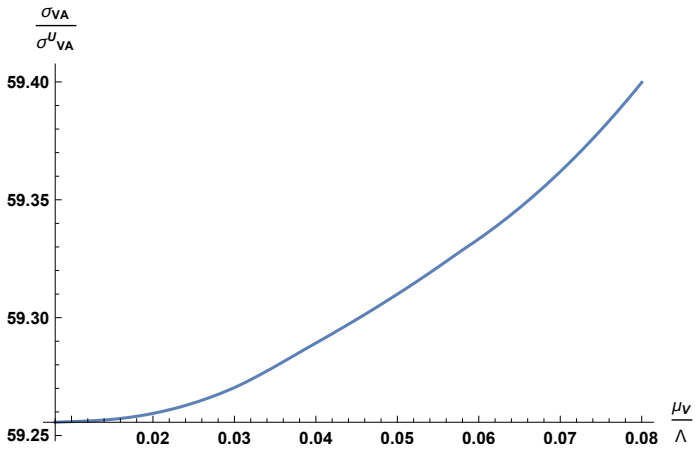

Figure 6.2: CSE radiative corrections as a function of μ_V with μ_A fixed. The conductivity is normalized by the universal conductivity, μ^U_{VA}.

6.2 Computation of Anomalous Conductivities

Similarly to the case in Chapter 5, we define the relevant sources through the asymptotic behaviour of δV_{x1}, δA_{x2} and δh_1. Precisely, the magnetic fields and vorticity are

$$\lim_{a\to\infty} \delta V_{x1} \sim -B_V + \hat{V} L^2 e^{-2a}, \tag{6.19}$$

$$\lim_{a\to\infty} \delta A_{x1} \sim -B_A e^{-\Delta a} L^{\Delta} a^{-p} + \hat{A} e^{(\Delta-2)a} a^{p}, \tag{6.20}$$

$$\lim_{a\to\infty} \delta h_1 \sim -\omega + \hat{h} L^2 e^{-2a} \tag{6.21}$$

respectively.

It is important to note that we will not be computing corrections to the universal values associated with the covariant current (2.20), the form in which they are usually presented. This stems from the fact that it is impossible to define a covariant current in the case where A_M is massive [49]. Therefore, the universal values that we will make reference to from this point onwards are [25]

$$\sigma_{VV} = 0 \quad , \quad \sigma_{VA} = \frac{\mu_V}{2\pi^2} \quad , \quad \sigma_{V\Omega} = 0. \tag{6.22}$$

Before actually computing the radiative corrections, we need to confirm if any of the chiral or vortical conductivites recieve corrections at all. This is not so straightforward as there is no analytical formula to work with. We only know that the response (6.13) should have the appearance of (2.16). Hence, by tweaking the values of the input parameters and the sources, we can deduce exactly which forms of anomalous response are present.

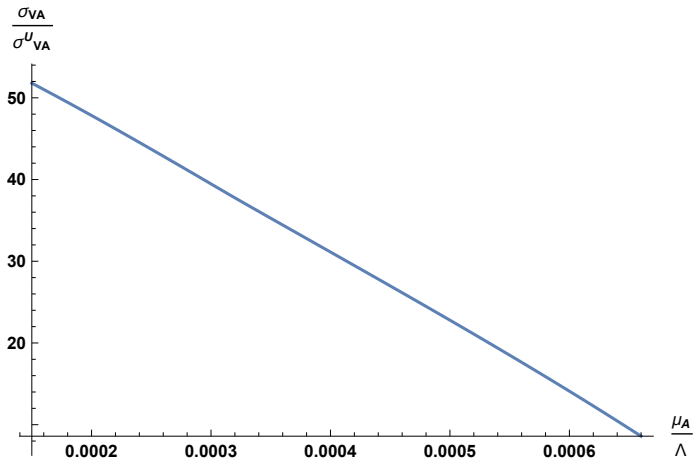

Figure 6.3: CSE radiative corrections as a function of μ_A with μ_V fixed. The conductivity is normalized by the universal conductivity, σ^U_{VA}.

We find that the CME and CVE are zero, thereby receiving no radiative corrections in accordance with (6.22). As is shown in Fig 6.1, the CSE is non-zero. Indeed, this has to be the case for our result to agree with the universal values (6.22). Whether or not the CSE receives corrections is a different question. It turns out that it does and we will spend the rest of the section attempting to identify such corrections.

As was mentioned in the previous chapter when discussing plots of the thermodynamic quantities, it is extremely difficult to fix the output values of the numerical solver, μ_V and μ_A. However, this is necessary to check the universal behaviour of the CSE[3]. While not visible in either Fig 6.2 or Fig 6.3, we find in the presence of constant μ_V, that σ^U_{VA} is constant. Furthermore, in the presence of constant μ_A, the dependence of σ_{VA} on μ_V is linear. This is a reassuring consistency check, implying that our model does produce the required universal behaviour (6.22) in the absence of the gluon anomaly.

We will finalize this section by providing a comparison of the figures 6.2 and 6.3. The function in Fig 6.2, while monotonically increasing has a very small derivative compared to that in Fig 6.3. In other words, the adjustment of μ_V seems to have a very small effect on the radiative corrections in comparison to that of μ_A. As we have seen before during the analysis of the holographic model, this stems from the massive nature of the field associated with μ_A.

The fact that μ_V is associated with a massless field allows us to probe a larger range of chemical potentials, although this is still not really large enough. Ideally, one would like to have access to both vector and chemical potentials

[3]The universal values for the conductivities are computed by turning off the mass term in the equations of motion, i.e sending $Z(\lambda) \to 0$.

$\gg 1$. However, the square root in the DBI action will contribute to numerical difficulties if the input unscaled charges $\tilde{Q}^V$, $\tilde{Q}^A$ are too large. We have found that the conductivity becomes negative if μ_A is further increased in Fig 6.3. This sheds a significant amount of doubt over the validity of the prediction as the corrections go to zero.

Chapter 7

Conclusion and Outlook

We have successfully built a holographic model, which enables us to compute radiative corrections to anomalous conductivities within the setting of the QGP. We summarize our main results below while also mentioning some aspects of the model that could be investigated further.

It is apparent that the key ingredient needed in the holographic model to produce dynamical gluons is a massive axial gauge field, A_M. The presence of this massive field intentionally induces an anomalous dimension, Δ associated with the current $\mathcal{J}_A^\mu$. Moreover, for the considered model to produce QCD, we must demand that $\Delta > -1$. It turns out that the constant Z_0 is intimately related to Δ. However, our original definition for $Z(\lambda)$ will not be able to produce a Δ satisfying this bound. We showed that by adding a linear term to the potential $Z(\lambda)$, this problem is seemingly fixed and for the purpose of the thesis, we chose $\Delta = -0.7$.

There are many avenues that one could pursue to expand on this analysis. First and foremost, it would be ideal to fix the coefficients c, d to some physical quantity associated with either lattice or experimental data. In the bulk theory, pseudoscalar gluballs are associated with fluctuations of the axionic field, $\delta\mathfrak{a}$. The fact that the potential $Z(\lambda)$ is holographically related to the spectrum of pseudoscalar glueballs [42] could then provide a mechanism for fixing such coefficients. In addition, it could be intructive to perform a comparison between our results and [25], where the fluctuations are organized in a perturbative expansion in Δ. A better understanding of the behaviour of the radiative corrections of the CSE as a function of Δ in general woud be desirable.

The thermodynamics of the holographic background were studied by plotting the temperature and chemical potentials as a function of the free parameter, λ_h. Perhaps, as should be expected, the massless field V_M does not backreact at all in comparison to A_M. From Fig 5.5, the nonmonotonic nature of the μ_A curves imply that there could be some kind of phase coexistence. To study this fur-

ther, one could make use of technology already provided by V-QCD [52]. It was mentioned in Chapter 4 that the justification to not include the tachyon comes from the fact that we are not considering the chiral condensate to be relevant for our analysis. Nonetheless, it might be interesting to include the tachyon if we want to incorporate chiral symmetry breaking into the phase structure of our model [43].

In Chapter 4, we made use of the holographic prescription to compute the current $\mathcal{J}_V^\mu$. One can just as easily compute the current $\mathcal{J}_A^\mu$ by functional differentiation of the on-shell gravitational action with respect to A_μ. Within the response to this current lies another anomalous conductivity, namely $\sigma_{\Omega A}$, associated with the CVSE. The CVSE has the special property, which is that its universal value only depends on temperature [8]. It is believed that for this reason, $\sigma_{\Omega A}$ is more likely to be observed in the QGP. This is because temperature is the only ingredient required to produce such an anomalous response, as opposed to the aforementioned conductivities, in which case the existence of a chiral medium is required. Computing $\delta\mathcal{J}_A^\mu$ is definitely a realistic goal. The only caveat is that one would then need to solve the full set of fluctuation equations, including the Chern-Simons terms.

The response to the current $\delta\mathcal{J}_A^\mu$ was computed numerically. Radiative corrections were found to be zero in the case of the CME and CVE, matching with the universal behaviour (6.22). We were also able to recover the universal value for the CSE by observing the lack of dependence of σ_{VA} on μ_V and linear dependence on μ_A. The radiative corrections were then studied for fixed μ_V and separately for μ_A. We have concluded that there are indeed radiative corrections to the CSE, although a more concrete understanding of the parameter space associated with the numerical solver will be needed to explore the behaviour properly.

Appendix A

Potential Definitions

In this appendix we give the coefficients of the potentials $V_g(\lambda), V_f(\lambda)$ and $w(\lambda)$ explicitly [54]. We do not explain the justification behind the choice of such coefficients as this was partly explained in chapter 4 as well. Lastly, we demonstrate how the coefficient Z_0 was computed from the work [53].

Potential Coefficients

For clarity's sake we recall the definitions here, starting with the gluonic potential

$$V_g(\lambda) = 12\left[1+V_1\lambda+\frac{V_2\lambda^2}{1+\lambda/\tilde{\lambda}_0}+V_{\rm IR}e^{-\tilde{\lambda}_0/\lambda}(\lambda/\tilde{\lambda}_0)^{4/3}\sqrt{\log\Big(1+\lambda/\tilde{\lambda}_0\Big)}\right]. \quad \text{(A.1)}$$

In addition, the potentials for the flavor sector are

$$V_f(\lambda) = W_0 + W_1\lambda + \frac{W_2\lambda^2}{1+\lambda/\tilde{\lambda}_0} + W_{\rm IR}e^{-\tilde{\lambda}_0/\lambda}(\lambda/\tilde{\lambda}_0)^2, \quad \text{(A.2)}$$

$$\frac{1}{w(\lambda)} = w_0\left[1+\bar{w}_0 e^{\hat{\lambda}_0/\lambda}\frac{(\lambda/\hat{\lambda}_0)^{4/3}}{\log\Big(1+\lambda/\hat{\lambda}_0\Big)}\right]. \quad \text{(A.3)}$$

We then choose to work with the definitions of the UV coefficients

$$\begin{aligned} V_1 &= \frac{11}{27\pi^2} \quad , \quad V_2 = \frac{4619}{46656\pi^4} \quad , \quad w_0 = 1.28 \\ W_0 &= 2.5 \quad , \quad W_1 = \frac{8+3W_0}{9\pi^2} \quad , \quad W_2 = \frac{6488+999W_0}{15552\pi^2}. \end{aligned} \quad \text{(A.4)}$$

Furthermore, the choice of IR coefficients is

$$V_{\rm IR} = 2.05 \quad , \quad \hat{\lambda}_0 = \frac{8\pi^2}{3} \quad , \quad W_{\rm IR} = 0.9.$$

Computation of Z_0

Recall the definition of Z_0 that produces the correct IR asymptotics, namely

$$Z(\lambda) = Z_0\Big(1 + c\frac{\lambda}{\tilde{\lambda}_0} + d\frac{\lambda^4}{\tilde{\lambda}_0^4}\Big), \tag{A.5}$$

with $\tilde{\lambda}_0 = 8\pi^2$. We compute Z_0 by making use of Eq 2.17 in [53]. After rewriting the equation in a coordinates and scaling, we arrive at the expression

$$Z_0 = -\int_0^{a_{\text{cut}}} da e^{-4(a+\delta_a)} \frac{q\chi}{\Big(1 + c\frac{\lambda}{\tilde{\lambda}_0} + d\frac{\lambda^4}{\tilde{\lambda}_0^4}\Big) M_p^3 \Lambda} \tag{A.6}$$

where χ is the topological susceptibility. Even though this is only supposed to be valid in the $T = 0$ regime, we can adapt our numerical solution to such a situation by taking λ_h to be very large ($\sim 10^6$). The numerical values of M_p, Λ and χ are taken from lattice data [53], [47] and their combination reads

$$\frac{\chi}{M_p^3 \Lambda} = \frac{45\pi^2}{1.3}\Big(\frac{191}{(1.28)(270)}\Big). \tag{A.7}$$

Appendix B

Holographic Equations of Motion

In this appendix, we list the full equations of motion for the holographic model (without assumption of any specific background or fluctuations). The equation of motion for V_M is

$$\frac{3}{4}\kappa\tilde{\epsilon}^{MNPQR}F^V_{MN}F^A_{PQ}=\partial_M\Big[\frac{xV_f(\lambda)w(\lambda)}{8}\sum_{k=+,-}\sqrt{-\det \boldsymbol{A}_k}\Big(\boldsymbol{A}_k^{-1RM}-\boldsymbol{A}_k^{-1MR}\Big)\Big], \tag{B.1}$$

while for A_M, it reads

$$\begin{aligned}&\tilde{\epsilon}^{MNPQR}(\frac{3}{4}\kappa F^V_{MN}F^V_{PQ}+2\gamma F^A_{MN}F^A_{PQ})=Z(\lambda)\sqrt{-g}g^{MR}(\partial_M\mathfrak{a}-2xA_M)\\&+\partial_M\Big[\frac{xV_f(\lambda)w(\lambda)}{8}\sum_{k=+,-}k\sqrt{-\det \boldsymbol{A}_k}\Big(\boldsymbol{A}_k^{-1RM}-\boldsymbol{A}_k^{-1MR}\Big)\Big].\end{aligned} \tag{B.2}$$

The Einstein equations are

$$\begin{aligned}R_{MN}=&-\frac{g_{MN}V_g(\lambda)}{3}+\frac{g_{MN}xV_f(\lambda)}{12\sqrt{-g}}\sum_{k=+,-}\sqrt{-\det \boldsymbol{A}_k}\mathrm{Tr}(\boldsymbol{A}_k^{-1})\\&+\frac{4}{3\lambda^2}\partial_M\lambda\partial_N\lambda-\frac{xV_f(\lambda)}{8\sqrt{-g}}\sum_{k=+,-}\sqrt{-\det \boldsymbol{A}}_k g_{MP}\Big(\boldsymbol{A}_k^{-1PQ}+\boldsymbol{A}_k^{-1QP}\Big)g_{QN}\\&+\frac{1}{2}Z(\lambda)(\partial_M\mathfrak{a}-2xA_M)(\partial_N\mathfrak{a}-2xA_N).\end{aligned} \tag{B.3}$$

Finally, the equations of motion for the dilaton and the axion are

$$\begin{aligned}\frac{\sqrt{-g}}{2}\frac{dZ(\lambda)}{d\lambda}(\partial_M\mathfrak{a}-2xA_M)^2 &= \frac{8}{3\lambda}\partial_M\Big[\frac{g^{MN}\sqrt{-g}\partial_N\lambda}{\lambda}\Big]+\sqrt{-g}\frac{dV_g(\lambda)}{d\lambda}\\ &-\frac{x}{2}\frac{dV_f(\lambda)}{d\lambda}\sum_{k=+,-}\sqrt{-\det\boldsymbol{A}_k}\\ &+\frac{1}{4}xV_f(\lambda)\frac{dw(\lambda)}{d\lambda}\sum_{k=+,-}\sqrt{-\det\boldsymbol{A}_k}\boldsymbol{A}_k^{-1MN}\Big(F^V_{MN}\pm F^A_{NM}\Big)\end{aligned} \tag{B.4}$$

and

$$0=\partial_M[g^{MN}\sqrt{-g}Z(\lambda)(\partial_N\mathfrak{a}-2xA_N)] \tag{B.5}$$

respectively.

Bibliography

[1] Matthew Dean Schwartz. *Quantum Field Theory and the Standard Model*. Cambridge University Press.

[2] Dmitri E. Kharzeev. The Chiral Magnetic Effect and Anomaly-Induced Transport. *Progress in Particle and Nuclear Physics*, 75:133–151.

[3] Shuo Wang, Ben-Chuan Lin, An-Qi Wang, Da-Peng Yu, and Zhi-Min Liao. Quantum transport in Dirac and Weyl semimetals: A review. *Advances in Physics: X*, 2(3):518–544.

[4] Matthias Kaminski, Christoph F. Uhlemann, Marcus Bleicher, and Jürgen Schaffner-Bielich. Anomalous hydrodynamics kicks neutron stars. *Physics Letters B*, 760.

[5] Dmitri E. Kharzeev, Larry D. McLerran, and Harmen J. Warringa. The effects of topological charge change in heavy ion collisions: "Event by event P and CP violation". *Nuclear Physics A*, 803(3-4):227–253.

[6] Observation of charge asymmetry dependence of pion elliptic flow and the possible chiral magnetic wave in heavy-ion collisions. *Physical Review Letters*, 114(25).

[7] A. Gynther, K. Landsteiner, F. Pena-Benitez, and A. Rebhan. Holographic Anomalous Conductivities and the Chiral Magnetic Effect. *Journal of High Energy Physics*, 2011(2):110.

[8] Karl Landsteiner, Eugenio Megias, Luis Melgar, and Francisco Pena-Benitez. Holographic Gravitational Anomaly and Chiral Vortical Effect. *Journal of High Energy Physics*, 2011(9):121.

[9] Makoto Natsuume. *AdS/CFT Duality User Guide*. Springer Japan.

[10] Karl Landsteiner. Notes on Anomaly Induced Transport. *Acta Physica Polonica B*, 47(12):2617.

[11] Pavel Kovtun. Lectures on hydrodynamic fluctuations in relativistic theories. *Journal of Physics A: Mathematical and Theoretical*, 45(47):473001.

[12] Eugenio Megias and Manuel Valle. Anomalous transport in second order hydrodynamics. *EPJ Web of Conferences*, 126.

[13] L.D. Landau and E.M Lifshitz. *Fluid Mechanics*. Permagon Press.

[14] Mikhail A. Stephanov and Ho-Ung Yee. No-Drag Frame for Anomalous Chiral Fluid. *Physical Review Letters*, 116(12):122302.

[15] D. T. Son and A. R. Zhitnitsky. Quantum Anomalies in Dense Matter. *Physical Review D*, 70(7):074018.

[16] Johanna Erdmenger, Michael Haack, Matthias Kaminski, and Amos Yarom. Fluid dynamics of R-charged black holes. *Journal of High Energy Physics*, 2009(01):055–055.

[17] Dam T. Son and Piotr Surowka. Hydrodynamics with Triangle Anomalies. *Physical Review Letters*, 103(19):191601.

[18] Kenji Fukushima, Dmitri E. Kharzeev, and Harmen J. Warringa. The Chiral Magnetic Effect. *Physical Review D*, 78(7):074033.

[19] Karl Landsteiner, Eugenio Megias, and Francisco Pena-Benitez. Anomalous Transport from Kubo Formulae. *Journal of High Energy Physics*, 871(5):81.

[20] Kristan Jensen, R. Loganayagam, and Amos Yarom. Thermodynamics, gravitational anomalies and cones. *Journal of High Energy Physics*, 2013(2):88.

[21] Umut Gursoy and Javier Tarrio. Horizon universality and anomalous conductivities. *Journal of High Energy Physics*, 2015(10):58.

[22] Sašo Grozdanov and Napat Poovuttikul. Universality of anomalous conductivities in theories with higher-derivative holographic duals. *Journal of High Energy Physics*, 2016(9):46.

[23] Kristan Jensen, Pavel Kovtun, and Adam Ritz. Chiral conductivities and effective field theory. *Journal of High Energy Physics*, 2013(10):186.

[24] Arata Yamamoto. Chiral magnetic effect in lattice QCD with a chiral chemical potential. *Physical Review Letters*, 107(3):031601.

[25] Angel Domingo Gallegos and Umut Gürsoy. Dynamical gauge fields and anomalous transport at strong coupling. *Journal of High Energy Physics*, 2019(5):1.

[26] Stephen L. Adler. Axial-Vector Vertex in Spinor Electrodynamics. *Physical Review*, 177(5):2426–2438.

[27] Kazuo Fujikawa. Path-Integral Measure for Gauge-Invariant Fermion Theories. *Physical Review Letters*, 42(18):1195–1198.

[28] Kazuo Fujikawa and Hiroshi Suzuki. *Path Integrals and Quantum Anomalies*. Oxford University Press.

[29] Adel Bilal. Lectures on Anomalies. *Laboratoire de Physique Theorique de I'ENS*.

[30] Stephen L. Adler and William A. Bardeen. Absence of Higher-Order Corrections in the Anomalous Axial-Vector Divergence Equation. *Physical Review*, 182(5):1517–1536.

[31] M. F. Atiyah and I. M. Singer. The index of elliptic operators on compact manifolds. *Bulletin of the American Mathematical Society*, 69(3):422–434.

[32] William A. Bardeen and Bruno Zumino. Consistent and covariant anomalies in gauge and gravitational theories. *Nuclear Physics B*, 244(2):421–453.

[33] D. E. Kharzeev, J. Liao, S. A. Voloshin, and G. Wang. Chiral Magnetic and Vortical Effects in High-Energy Nuclear Collisions — A Status Report. *Progress in Particle and Nuclear Physics*, 88:1–28.

[34] L. Susskind. The World as a Hologram. *Journal of Mathematical Physics*, 36(11):6377–6396.

[35] Juan M. Maldacena. The Large N Limit of Superconformal Field Theories and Supergravity. *International Journal of Theoretical Physics*, 38(4):1113–1133.

[36] Jorge Casalderrey-Solana, Hong Liu, David Mateos, Krishna Rajagopal, and Urs Achim Wiedemann. *Gauge/String Duality, Hot QCD and Heavy Ion Collisions*. Cambridge University Press.

[37] Martin Ammon and Johanna Erdmenger. *Gauge/Gravity Duality: Foundations and Applications*. Cambridge University Press.

[38] S. S. Gubser, I. R. Klebanov, and A. M. Polyakov. Gauge Theory Correlators from Non-Critical String Theory. *Physics Letters B*, 428(1-2):105–114.

[39] Umut Gursoy. Improved Holographic QCD and the Quark-gluon Plasma. *Acta Physica Polonica B*, 47(12):2509.

[40] O. Aharony, S. S. Gubser, J. Maldacena, H. Ooguri, and Y. Oz. Large N Field Theories, String Theory and Gravity. *Physics Reports*, 323(3-4):183–386.

[41] T. Alho, M. Jarvinen, K. Kajantie, E. Kiritsis, and K. Tuominen. On finite-temperature holographic QCD in the Veneziano limit. *Journal of High Energy Physics*, 2013(1):93.

[42] U. Gursoy and E. Kiritsis. Exploring improved holographic theories for QCD: Part I. *Journal of High Energy Physics*, 2008(02):032–032.

[43] Roberto Casero, Elias Kiritsis, and Angel Paredes. Chiral symmetry breaking as open string tachyon condensation. *Nuclear Physics B*, 787(1-2):98–134.

[44] Matti Jarvinen and Elias Kiritsis. Holographic Models for QCD in the Veneziano Limit. *Journal of High Energy Physics*, 2012(3):2.

[45] G. Veneziano. U(1) without instantons. *Nuclear Physics B*, 159(1-2):213–224.

[46] M. A. Shifman, A. I. Vainshtein, and V. I. Zakharov. QCD and resonance physics. theoretical foundations. *Nuclear Physics B*, 147(5):385–447.

[47] Niko Jokela, Matti Jarvinen, and Jere Remes. Holographic QCD in the Veneziano limit and neutron stars. *Journal of High Energy Physics*, 2019(3):41.

[48] Marco Panero. Thermodynamics of the QCD plasma and the large-N limit. *Physical Review Letters*, 103(23):232001.

[49] Amadeo Jimenez-Alba, Karl Landsteiner, and Luis Melgar. Anomalous Magneto Response and the Stuckelberg Axion in Holography. *Physical Review D*, 90(12):126004.

[50] Ioannis Papadimitriou and Kostas Skenderis. AdS/CFT correspondence and Geometry. *IRMA Lectures in Mathematical and Theoretical Physics*, 8:73–101, 2005.

[51] Dongsu Bak, Andreas Karch, and Laurence G. Yaffe. Debye screening in strongly coupled N=4 supersymmetric Yang-Mills plasma. *Journal of High Energy Physics*, 2007(08):049–049.

[52] T. Alho, M. Jarvinen, K. Kajantie, E. Kiritsis, C. Rosen, and K. Tuominen. A holographic model for QCD in the Veneziano limit at finite temperature and density. *Journal of High Energy Physics*, 2014(4):124.

[53] Umut Gursoy, Ioannis Iatrakis, Elias Kiritsis, Francesco Nitti, and Andy O'Bannon. The Chern-Simons Diffusion Rate in Improved Holographic QCD. *Journal of High Energy Physics*, 2013(2):119.

[54] Takaaki Ishii, Matti Järvinen, and Govert Nijs. Cool baryon and quark matter in holographic QCD. *Journal of High Energy Physics*, 2019(7):3.